PENTLANDITE PHASE RELATIONS IN THE FE-NI-S SYSTEM AND THE STABILITY OF THE PYRITE-PENTLANDITE ASSEMBLAGE

by

R. W. Shewman

A thesis submitted to the Faculty of Graduate Studies and Research of McGill University in partial fulfilment of the requirements for the degree of Master of Science.

Department of Geological Sciences

McGill University

June, 1966

© R.W. Shewman 1967

Short Thesis Title

Phase Relations in the Pentlandite Region of the Fe-Ni-S System

PENTLANDITE PHASE RELATIONS IN THE FE-NI-S SYSTEM AND THE STABILITY OF THE PYRITE-PENTLANDITE ASSEMBLAGE

Abstract

Phase relations in part of the Fe-Ni-S system were investigated between 200 and 600°C with emphasis on the pentlandite region and the pyrite-pentlandite join.

An x-ray determinative curve for synthetic pentlandite was determined experimentally as follows: $y = 1.9407 - 0.0023x + 0.0077x^2$, where "y" represents the d_{115} value in Å and "x" represents the iron to nickel weight ratio. The following iron, nickel and sulphur solid solubility limits of pentlandite were determined.

	Fe : Ni weight ratio	wt % Sulphur
600°C	1.12 ± 0.04 to 0.63 ± 0.03	32.55 ± 0.20 to 34.00 ± 0.30
500°C	1.67 ± 0.04 to 0.38 ± 0.04	32.95 ± 0.25 to 33.90 ± 0.20
400°C	1.88 ± 0.04 to 0.62 ± 0.07	32.95 ± 0.20 to 33.55 ± 0.25

The upper stability limit of the pyrite-pentlandite assemblage was determined as 230 ± 30°C in the presence of the equilibrium vapor.

X-ray powder patterns of monosulphide solid solution heated at 500 and 400°C with a composition (wt %) of 18.8 Fe, 43.8 Ni, and 37.4 S showed a modulated structure. A solvus interrupts the monosulphide solid solution below about 300°C. Approximate solvus limits in atomic per cent nickel are:

250°C	19%	36%
200°C	12%	38%

ACKNOWLEDGMENTS

The author wishes to thank Drs. L. A. Clark, A. J. Frueh and G. R. Webber for use of their laboratory facilities and for guidance in the course of the experimental study.

I am especially grateful to Dr. L. A. Clark for suggesting the problem, for supervising the research and for reviewing the manuscript.

In addition to many of the above laboratory facilities, I am also indebted to the National Research Council for financial support through Operating Grant A-1111, held by Dr. L. A. Clark.

TABLE OF CONTENTS

TABLE OF CONTENTS

TABLES

Appendix

FIGURES

FIGURES

Continued

Appendix

PLATES

CHAPTER I

INTRODUCTION

In the last decade geologists have made increasing use of phase equilibrium studies in synthetic systems to provide the fundamental data for the interpretation and understanding of the occurrence of minerals and mineral assemblages. The economic geologist has directed considerable study into the phase relations of the Fe-Ni-S system as a large number of the phases are found as minerals, which in some cases constitute important sources of nickel, iron and related metals.

Most of the work in the Fe-Ni-S system has been carried out by D. G. Kullerud and others of the Carnegie Institute of Washington. From a detailed investigation into the related binary systems, and limited synthetic studies of the ternary phase relations, Kullerud (1963) was able to formulate the phase relations in the Fe-Ni-S system on ten isothermal sections. The results of this work provided geologists with data directly applicable to mineral assemblages in ores and meteorites, although most of the phase relations were not worked out in detail. Dr. L. A. Clark had noted some uncertainties in the synthetic phase relations in the region of pentlandite which warrented additional experimental work. Numerous inconsistencies are also present in the literature in regard to the solubility limits of pentlandite. The immediate purpose of the writer's investigation

was to determine the iron, nickel, and sulphur solubility limits of pentlandite at geologically interesting temperatures; and to determine the upper stability limit of the pyrite-pentlandite assemblages.

Since this assemblage is not uncommon in nickel sulphide deposits, and since its upper stability limit was not closely defined by Kullerud (1963), its determination would give an important clue as to the physical environment of formation of some of the minerals in nickel deposits.

CHAPTER II

PREVIOUS WORK

Chemical Composition and Crystal Structure of Pentlandite

The mineral pentlandite has been known since 1843 when Scheerer described its occurrence at Lillehammer, Norway. The composition of pentlandite was in doubt for some time due in large part to its association with finely admixed pyrrhotite in natural ores. Penfield (1893), in a study on the pentlandite from Sudbury, found the ratio of S : (Fe, Ni) almost exactly 1:1. Dickson (1903) found, from three analyses of Sudbury pentlandites, that the metals were present in proportions too large for the chemical formula (Ni, Fe)S. To accommodate his results he proposed the formula $(Fe, Ni)_{11}S_{10}$. Alsén (1925) proposed a crystal structure based on a hexagonal cell with a space group O_h^5 - Fm3m, taking the number of atoms per unit cell as 64, and the corresponding formula (Fe, Ni)S.

Newhouse (1927) determined the melting point of Sudbury pentlandite as 878°C, and noted that the temperature range suggests it is a solid solution in which the iron to nickel ratio varies. Pentlandite on melting was found to break up into two components, pyrrhotite and a nickel sulphide which he tentatively identified as Ni_3S_2. Newhouse successfully synthesized pentlandite by melting Fe, Ni, and S in a graphite crucible, with repeated additions of S until the desired product was obtained.

Metallurgical studies in the Fe-Ni-S system by Bornemann (1908, 1910), Vogel and Tonn (1930), Guertler and Savelsberg (1932) and Urazov and Filin (1938) reported the compound $2FeS.Ni_3S_2$ which Colgrove (1942) showed to be a member of the pentlandite solid solution series.

Zurbrigg (1933) prepared synthetic pentlandite from melts ranging in composition from 45FeS:55NiS to 10FeS:90NiS, which correspond to a field in which the Fe:Ni weight ratio varies from 0.11 to 0.80.

From an x-ray powder study, Lindqvist et al. (1936) showed that pentlandite was isostructural with synthetic Co_9S_8, and consequently wrote its formula as $(Fe,Ni)_9S_8$. The sulphide was shown to have a space group of O_h^5 - Fm3m, with four formula units M_9S_8 per unit cell. This crystal structure was later confirmed by Pearson and Buerger (1956), Knop and Ibrahim (1961) and Géller (1962). In an attempt to synthesize pure pentlandite of composition $Fe_{4,5}Ni_{4,5}S_8$ and $Fe_6Ni_3S_8$ Lindqvist et al. found in x-ray powder photographs, besides pentlandite, faint lines of pyrrhotite. Although pentlandite had been successfully synthesized, the limits of its solid solution remained undefined.

Colgrove (1942) showed that discrepancies in the results of previous investigators were in large part due to the "open" nature of their systems with respect to sulphur. By the use of pressure bombs and sealed glass tubes, Colgrove was able to resolve these discrepancies and to establish the phase relations in the region of the FeS-NiS section. Colgrove synthe-

sized most of his charges at temperatures above 630°C and allowed the runs to cool slowly to room temperature. Colgrove found that pentlandite had a range of composition in which the Fe : Ni weight ratio varies from 0.33 to 1.19, with a nearly constant sulphur content of 33 weight per cent.

Lundqvist (1947) investigated the Fe-Ni-S system by quartz tube quench experiments at three isothermal sections, 200, 400 and 680°C. From an x-ray study of the quench products he found that there was no variation in the lattice constant of pentlandite with the sulphur content of the samples, and stated the sulphur content as 47.0 atomic per cent (33.2 weight per cent), irrespective of the total sulphur content of the samples or of the temperature of the experiment. The stability limits of pentlandite were found to extend from a Fe : Ni weight ratio of 0.72 ± .01 to 1.37 ± .01, irrespective of the temperature from which the charges were rapidly cooled.

Eliseev (1955) reviewed 35 analyses of pentlandite and found that the weight ratio of Fe : Ni varied from 0.48 to 2.86, and the sulphur content from 38 to 43 atomic per cent. To accommodate these analyses he proposed the formula $Fe_4^{[4]}Ni_4^{[4]}(Co, Ni, Fe)^{[6]}_{0-1.0}S_8$ where the superscript 4 refers to tetrahedral and 6 to octahedral co-ordination. This formula provides for a variable Fe : Ni weight ratio of 0.76 to 1.19, as well as for a variable M : S ratio of 1 to 1.125. Knop et al. (1965) pointed out that not one of Chirkov's analyses, which Eliseev considered reliable, gives a

M:S ratio less than 1.15. The formula also does not account for the large spread in Fe:Ni ratios which Eliseev reported in his paper. Thus Eliseev's formula fails to accommodate the pentlandite analyses which his paper set out to explain.

Kullerud (1956) reported that preliminary quench experiments at 500°C in the Fe-Ni-S system indicated that pentlandite had an Fe:Ni weight ratio varying from 0.65 to 1.51, and a M:S ratio of 1.125 to 1.121.

Knop and Ibrahim (1961) found from sintering experiments that the saturation limits of pentlandite were $Fe_{6.8}Ni_{2.2}S_8$ and $Fe_{2.6}Ni_{6.4}S_8$ corresponding to a Fe:Ni weight ratio of 0.39 to 2.94.

Kullerud (1963) compiled the results of previous workers with those of his fellow workers at the Geophysical Laboratory and was able to show the phase relations of the Fe-Ni-S system at 10 different temperatures from 400 to 1100°C. From Kullerud's synthesis the following points are of importance to the writer's study on the pentlandite field of solid solution.

1. At 500°C, pentlandite forms a limited solid solution field with the Fe:Ni weight ratio varying from about 0.9 to 1.1, and the weight per cent S from about 32.5 to 33.8.

2. At 400°C, pentlandite forms a limited solid solution field with the Fe:Ni weight ratio varying from about 0.9 to 1.1, and the weight per cent S from about 32.7 to 33.6.

The above solubility limits were estimated from Kullerud's phase diagrams and must be considered approximate.

Kullerud (1963) studied the thermal stability of pentlandite by quenching, differential thermal analysis (D.T.A.) and high temperature x-ray diffraction experiments. Synthetic pentlandite of $Fe_{4.5}Ni_{4.5}S_8$ composition was found to decompose at 610 ± 2°C to two solid phases, $(Fe,Ni)_{1-x}S$ plus a high-temperature non-quenchable phase equivalent to $Ni_{3-x}S_2$. A composition equivalent to synthetic pentlandite began to melt at 862°C, yielding a metal-rich iron-nickel-sulphur liquid (~20 wt per cent S). Pentlandite from the Frood Mine, Sudbury, decomposed at 613°C and began to melt between 864° and 881°C. The breakdown of pentlandite at 610 ± 2°C is geologically important as many ores containing pentlandite are believed to have formed well above 600°C. Therefore, pentlandite must have formed as a phase during the cooling of the ore bodies.

In powder patterns of synthetic $Fe_{4.5}Ni_{4.5}S_8$ taken at 600°C, Kullerud observed a large increase in the cell edge which far exceeded that of any other investigated sulphide. In 1964 Morimoto and Kullerud determined the variation of unit-cell length of pentlandite of $Fe_{4.5}Ni_{4.5}S_8$ composition as a function of temperature from 25 to 608°C.

Bell et al. (1964) conducted high-pressure D.T.A. experiments on synthetic pentlandite of $Fe_{4.5}Ni_{4.5}S_8$ composition to determine the effect

of pressure on the temperature of breakdown. These D. T. A. experiments, over a pressure range of 400 to 36000 bars, showed that the breakdown temperature of pentlandite decomposed into pyrrhotite plus beta heazlewoodite at a temperature of about 425°C.

Popova et al. (1964) studied the fusion and crystallization of natural pentlandite. They found that natural pentlandite of composition $Fe_{9.4}Ni_{8.6}S_{16}$ melted incongruently, dissociating into pyrrhotite containing some nickel in solid solution and into a nickel-rich residual melt. In the pentlandites synthesized from the fusion of an ore concentrate, the metal to sulphur ratio was approximately 9:8 and the Fe:Ni weight ratio varied from 1.06 to 1.23.

Knop et al. (1965) reviewed all the available analyses of natural pentlandite, and of the 79 analyses found, 50 were sufficiently complete to study the stoichiometry of pentlandite. The Fe:Ni weight ratios of 49 low cobalt pentlandites ranged from about 0.63 to 4.75. If doubtful analyses are disregarded, pentlandites have Fe:Ni weight ratios varying from 0.81 to 1.12 which are amply provided for by Eliseev's formula. High cobalt pentlandites, however, are far outside the composition range permitted by Eliseev's formula, but the Fe:Ni weight ratios are all within 0.74 to 1.36, in spite of the strong variation in their cobalt content. The arithmetic average of 26 reliable analyses gives a M:S ratio of 1.13 ± 0.04 which is slightly higher than the ideal M:S ratio of 9:8 = 1.125.

Assuming that the pentlandites were homogeneous, the average composition does not correspond exactly with the formula M_9S_8 but is slightly higher in metal. Preliminary synthetic experiments by Knop et al. show a narrow homogeneity range from 33.2 to 32.7 weight per cent S, corresponding to the formula $(Fe,Ni)_9S_{8-X}$ $(0 \leqq X \leqq 0.2)$.

Knop et al. noticed that the unit cell dimensions of natural pentlandite are lower than the values obtained with synthetic samples. When natural pentlandites were annealed in vacuo at temperatures between 360 and 390°C, the lattice parameter increased into the range of values of synthetic pentlandite. Detailed studies on Creighton mine pentlandite showed that the lattice expansion was irreversible and took place between 150 and 200°C. The expansion was not prevented from taking place by argon pressures up to 2000 atm. Knop et al. suggested that the lattice expansion could be caused by geometrical ordering in the metal sublattices, i.e., order in the 32 (f) sublattice in the untreated state and statistical distribution in the annealed state.

As seen from Table 1, the composition of synthetic pentlandite varies considerably, and in some cases differs greatly from the solubility limits of natural pentlandite. The experimental results of all previous workers, excluding Kullerud and Lundqvist , are of questionable value since their experiments were not conducted on isothermal sections. The results of Lundqvist and of Kullerud are based on a limited number of

TABLE 1

CHEMICAL COMPOSITION OF PENTLANDITE

Fe : Ni wt Ratio	wt % S	M : S Atomic Ratio	Remarks, References.
(a) Theoretical Pentlandite of $Fe_{4.5}Ni_{4.5}S_8$ Composition			
0.951	33.23	1.125	
(b) Natural Pentlandite			
0.76-1.19		1.0-1.25	Eliseev (1955)
0.81-1.12		1.13 ± 0.04	Knop et al. (1965)
(c) Synthetic Pentlandite			
0.11-0.80			Zurbrigg (1933)
0.33-1.19	33		Colgrove (1942)
0.72 ± 0.01 to 1.37 ± 0.01	33.2		Lundqvist (1947)
0.65-1.51		1.121-1.125	Kullerud (1956)
0.39-2.94			Knop & Ibrahim (1961)
0.9 -1.02	32.5-33.4		600°C)
0.9 -1.1	32.5-33.8		500°C) Kullerud (1963)
0.9 -1.05	32.7-33.6		400°C)
1.06-1.23		1.125	Popova et al. (1964)
	32.7-33.2		Knop et al. (1965)

experiments, and since their experimental data were not published, a detailed appraisal is impossible.

$Fe_{1-x}S$ ---$Ni_{1-x}S$ Solid Solution Series

The end members in the $Fe_{1-x}S$ --- $Ni_{1-x}S$ series were studied by a number of researchers working along the binary Fe - S and Ni - S systems. Kullerud and Yoder (1959), and Kullerud and Yund (1962) summarize this previous work and present the results of their studies on the Fe - S and Ni - S systems.

The $Ni_{1-x}S$ phase occurs in two crystallographic modifications, the low-temperature, rhombohedral millerite (or β) form, and the high-temperature, hexagonal (or α) form with niccolite-type structure. The $\alpha \rightleftharpoons \beta$ inversion temperature varies from 379 $\pm$ 3°C for stoichiometric NiS, to 282 $\pm$ 3°C for $Ni_{1-x}S$ with maximum nickel deficiency of 2.18 weight per cent Ni (Kullerud and Yund, 1962). Nickel sulphide of the hexagonal NiAs structural type forms an omission type solid solution series (Arnold and Kullerud, 1956).

Natural and synthetic pyrrhotites ($Fe_{1-x}S$) possess three structural modifications:

1. Above the beta transformation at about 315°C (Roberts, 1935), rapidly cooled pyrrhotite ranging in composition from about 48.8 to 46.7 atomic per cent iron displays a hexagonal cell

with a 2A, 7C supercell structure (Desborough and Carpenter, 1965).

2. Below 315°C, hexagonal pyrrhotite (a = 2A, c = 5C) is present in the composition range 47.2 to 50.0 atomic per cent iron, and
3. monoclinic pyrrhotite (a = 2B, b = 2A, c = 4C) occurs at a composition of 46.67 atomic per cent iron (Fe_7S_8) (Desborough and Carpenter, 1965).

Substitutional solid solution between $Fe_{1-x}S$ and $Ni_{1-x}S$ yields a complete series which is referred to here as the monosulphide solid solution (Mss) of the Fe-Ni-S system.

The Mss field was first studied in detail by Zurbrigg (1933) who melted mixtures of FeS and NiS covering the entire section. He concluded that FeS may take up to 15 per cent NiS in solid solution. Zurbrigg's results are of limited value due to the unavoidable escape of sulphur during fusion which placed the bulk composition of the majority of runs in the metal-rich region below the Mss field.

Colgrove (1940) studied the FeS - NiS section but again the loss of sulphur from his charges resulted in a section with the metal : sulphur ratio greater than unity. In 1942 Colgrove restudied the Mss field, this time keeping the sulphur content constant by using sealed glass tubes and pressure bombs. Colgrove concluded that there is a complete

series between alpha solid solution ($NiS_{0.83}$ to $NiS_{1.08}$) and pyrrhotite solid solution ($FeS_{1.18}$ to FeS). He noted that there was a sudden change in the axial ratio of Mss between molar ratios Fe:Ni of 1:0.73 to 1:1.0. The significance of this change was not fully appreciated.

Lundqvist (1947) conducted an x-ray study on the quench products from silica tube experiments at 200, 480, and 680°C in the Fe-Ni-S system. He found that above 396°C the Mss field was complete between $Fe_{1-x}S$ and $Ni_{1-x}S$. Below 396°C a divariant field containing Mss and millerite separates Mss from NiS. At 200°C the nickel-rich limit of the Mss field is still very close to NiS, viz. at about 4 atomic per cent Fe and 46 atomic per cent Ni.

Quenching experiments by Kullerud (1956, 1963) indicated that the monosulphide solid solution is complete between $Fe_{1-x}S$ and $Ni_{1-x}S$ in the temperature range 992°C to about 525°C. At 500°C a narrow solubility gap was found in the Mss field at a composition of about 38 weight per cent Fe and 23 weight per cent Ni. Between 500 and 400°C this solubility gap had widened considerably so that tie lines became stable between pyrite and pentlandite at about 450°C.

Clark (1965) found that Mss with a composition of about 38 weight per cent Fe and 23 weight per cent Ni failed to break down into pyrite plus pentlandite when heated for periods up to 30 days at temperatures between 500 and 100°C. As these results cast some doubt on the validity of

Kullerud's findings, the writer's investigation was initiated to study the $Fe_{1-x}S$ --- $Ni_{1-x}S$ section for solubility gaps and the stability of the pyrite-pentlandite assemblage.

CHAPTER III

METHODS OF INVESTIGATION

Materials

Iron was obtained from the United Mineral and Chemical Corp., New York. The material was received as rods 1/4" X 6" containing 99.95 per cent Fe according to the producer's analysis. The analysis of this material showed it to contain impurities of 0.03 per cent carbon, 0.01 per cent oxygen and 0.01 per cent nitrogen. Seven other elements were reported in the ppm range.

Nickel, in rod form and of 99.99 per cent purity, was obtained from A.D. Mackay Inc., New York. A spectrographic analysis of this material indicated that the principal contaminants were 15 ppm silicon, 10 ppm iron, 3 ppm aluminum, 3 ppm copper, 2 ppm magnesium, 1 ppm calcium, and less than 1 ppm for manganese and silver.

Crystalline sulphur 99.999 per cent pure was obtained from the American Smelting and Refining Company.

The iron and nickel rods were filed to a powder of about 100 mesh and stored in an evacuated dessicator.

Techniques

A. Quench Experiments

1. Methods of synthesis

All of the runs were performed in simple sealed tubes of transparent, fused, silica glass. The suitability of silica glass as well as the evacuation and sealing techniques are described by Clark (1959, pp. 8-10).

Elements or previously synthesized compounds were loaded into silica glass tubes by a method of addition, using glass funnels of different lengths to nullify the adherence of reagents to the walls of the tubes. All weighing was done on a Mettler semi-micro "gram-atic" balance, permitting an accuracy of $\pm .02$ mg per weighing. In most cases at least 200mg of charge was used in each run, and the uncertainty in the composition, therefore, did not exceed 0.05 weight per cent. Loss of material to the vapor phase was effectively reduced by placing closely fitting silica glass rods over the charge before evacuating and sealing.

The majority of runs were quenched in cold water after a few days heating in a furnace, ground under acetone in an agate mortar to -100 mesh, inserted in a new tube, and reheated. Such grinding homogenizes the sample and shortens the additional time period needed to achieve equilibrium. The loss of material during the process of opening the tubes, grinding the contents, and loading new tubes was generally less

than 2.0 weight per cent. It was assumed that this small loss coincided in composition with that of the bulk. After the completion of each experiment the silica tubes were removed from the furnace using long tongs and were plunged rapidly into a cold water bath where they cooled to room temperature in a few seconds.

2. Temperature control and measurement.

Runs were heated in horizontal, cylindrical electric furnaces designed by Dr. G. Kullerud (with Wheatstone bridge-type control mechanism) (Clark, 1959, pp. 11-12). These furnaces maintain a constant temperature within $\pm$ 1°C over a 3.5 to 5 inch zone measured at 600°C. Temperatures were controlled to within $\pm$ 1 or $\pm$ 5°C, depending on the requirement of the experiment. Temperatures were measured with chromelalumel thermocouples and were recorded continuously on a multichannel recording potentiometer. Temperatures were periodically checked with a Rubicon potentiometer using a reference junction of 0°C.

3. Identification of the products.

a) Reflecting microscope: A representative portion of each charge was placed in a 1/4" steel press with some Acrylic Dental plastic. After squeezing in a vice for approximately five minutes, the hardened plastic pellet was extruded from the press and fastened to a glass slide with

vynilite. The polishing was first done dry on various grades of emery paper and then wet, using a gamma alumina suspension (Fisher, Grade B) on a "Gamel" polishing cloth mounted on a glass plate. All polished sections were examined under the reflecting microscope using an oil immersion objective lense of 60 power. Less than one tenth of one per cent of a phase with distinctive optical properties could readily be detected. Optically similar phases were readily distinguished after the section was stained with a dilute chromic acid solution.

b) X-ray diffraction: A portion of the charge was used for x-ray testing, and the remainder was stored in a plastic vial.

For qualitative work, the Guinier forward reflection, focussing, multiple exposure powder camera was found to be quite useful because this camera was able to show the presence of very small amounts of some phases (less than 1/2 wt per cent in some cases). Using Co-radiation, exposures of six hours at 20 KV and 10 mA were necessary. Some qualitative work was performed using a Phillips X-ray diffractometer. The powered charge to be tested was smeared on a glass slide with acetone. This mount was then rotated from 30 to 80^{o} 2θ using Fe-radiation at 40 KV and 10 mA. Those crystalline phases present in sufficient quantity to give reflections with intensities greater than the background intensity were then identified from the diffraction pattern.

Interplanar spacings were measured by mixing an internal standard

substance with the sample before mounting on either the Phillips X-ray diffractometer or the Guinier powder camera. NaCl (a=5.6402Å), LiF (a=4.0270Å) and Si (a=5.4282Å) were used as standards. To study the change in interplanar values of selected reflections the diffractometer was set to oscillate at least four times over the region to be measured using a goniometer speed of 1/4 degree per minute and a chart speed of one inch per degree. The reflections were measured at their centres of gravity which were visually estimated. The centres of the standard and unknown peaks were measured to $\pm$ 0.01° 2θ.

B. High Temperature X-ray Powder Diffraction

A Rigaku-Denki high temperature X-ray powder diffraction camera was used to determine the approximate breakdown temperature of synthetic pentlandite, and the non-quenchable high temperature products of this breakdown. A temperature controller, based on the wheatstone bridge principle, was used to regulate the temperature and to maintain the temperature within $\pm$ 2°C for the duration of the exposure. The temperature of the sample was determined from a calibration curve developed by Cabri (1964, p. A6). The sample was ground under acetone to -200 mesh and placed in a sealed, evacuated, silica glass capillary with a wall thickness of 0.01 mm. and outside diameter of 0.3 mm. During the exposure the camera was continuously evacuated and the temperature dis-

tribution in the furnace kept uniform by a flow of cooling water. Using iron radiation, exposure times of up to 16 hours duration were necessary at 40 KV and 10 mA. With Cu K_{α_1} radiation, exposure times of 3 to 4 hours duration at 35 KV and 20 mA were sufficient.

CHAPTER IV

EXPERIMENTAL RESULTS

Introduction

The phase relations in the central portion of the Fe-Ni-S system at 600, 500 and 400°C are shown in Figures 1, 2 and 3 respectively. Many parts of these phase diagrams were taken from the work of Clark and Kullerud (1963) and Kullerud (1963). The writer's interpretation is based on silica tube quench experiments in the region of the pentlandite solid solution field and the monosulphide solid solution series. The bulk compositions of some experiments conducted in this study are shown on each isothermal section, and a detailed account of the composition, thermal history and observations is given in the appendix.

A prominent feature of the phase relations in the central portion of the Fe-Ni-S system at the isothermal sections shown is the field of complete solid solution between $Fe_{1-x}S$ and $Ni_{1-x}S$. Kullerud (1963) had previously reported that this monosulphide solid solution series (Mss) was incomplete below about 450°C. As will be discussed in detail later, the writer's results suggest that the formation of two immiscible Mss phases is not reached until about 270°C. As a consequence, the pyrite-pentlandite tie line cannot form in the presence of vapor at a temperature above 270°C and in fact, as will be shown later, it is found to form at 230 ± 30°C.

Key to Figures 1, 2, and 3

Phases present in equilibrium with vapor

1. py + liquid
2. py + vs + liquid
3. vs + liquid
4. py + Mss
5. py + vs + Mss
6. vs + Mss
7. Mss
8. Mss + pn
9. Mss + pn + $\propto Ni_7S_6$
10. Mss + $\propto Ni_7S_6$
11. $\propto$(Fe,Ni) + po
12. $\propto$(Fe,Ni) + γ(Fe,Ni) + po
13. γ(Fe,Ni) + po
14. pn + po + γ(Fe,Ni)
15. pn + γ(Fe,Ni)
16. pn + γ(Fe,Ni) + $FeNi_3$
17. pn + $FeNi_3$
18. pn + $FeNi_3$ + hz
19. pn + hz
20. pn + hz + $\propto Ni_7S_6$
21. pn + $\propto Ni_7S_6$
22. hz + $\propto Ni_7S_6$
23. hz + $FeNi_3$
24. hz + $FeNi_3$ + γ(Fe,Ni)
25. hz + γ(Fe,Ni)
26. po + $(Ni,Fe)_{3\pm x}S_2$ + γ(Fe,Ni)
27. po + $(Ni,Fe)_{3\pm x}S_2$
28. po + $(Ni,Fe)_{3\pm x}S_2$ + pn
29. pn + $(Ni,Fe)_{3\pm x}S_2$
30. pn + $(Ni,Fe)_{3\pm x}S_2$ + Mss
31. $(Ni,Fe)_{3\pm x}S_2$ + Mss
32. $(Ni,Fe)_{3\pm x}S_2$ + γ(Fe,Ni)
33. $(Ni,Fe)_{3\pm x}S_2$ + γ(Fe,Ni) + pn

Symbols

pn = pentlandite = $(Fe,Ni)_9S_8$

po = pyrrhotite = $Fe_{1-x}S$

vs = vaesite = NiS_2

py = pyrite = FeS_2

hz = heazlewoodite = Ni_3S_2

Mss = monosulphide solid solution

$FeNi_3$ = awaruite

(Fe,Ni) = iron-nickel alloy

FeS = troilite

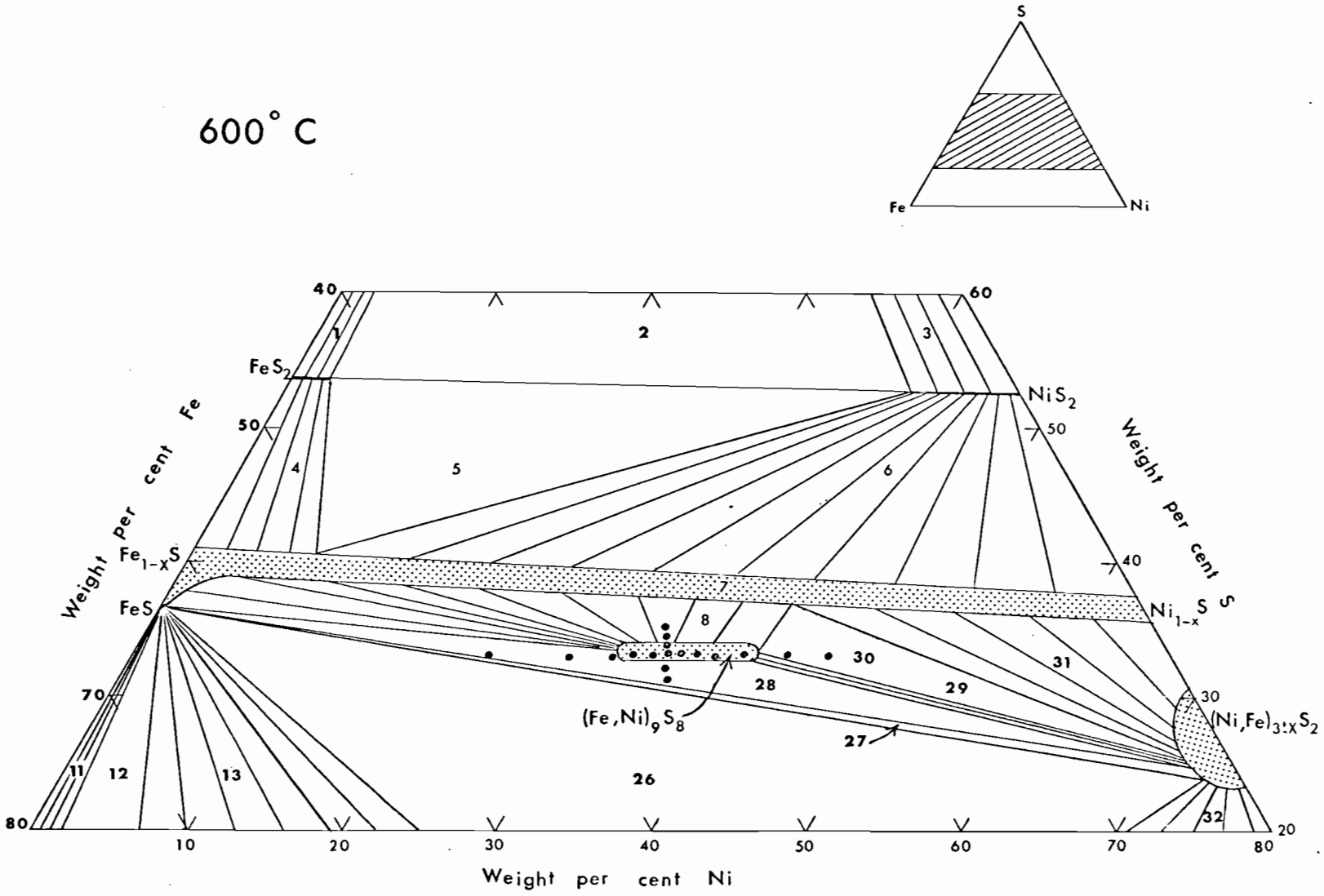

Figure 1. Phase relations in the central portion of the Fe-Ni-S system at 600°C in equilibrium with vapor. Solid circles represent bulk compositions of some runs at 600°C.

Key to Figures 1, 2, and 3

Phases present in equilibrium with vapor

1. py + liquid
2. py + vs + liquid
3. vs + liquid
4. py + Mss
5. py + vs + Mss
6. vs + Mss
7. Mss
8. Mss + pn
9. Mss + pn + $\propto Ni_7S_6$
10. Mss + $\propto Ni_7S_6$
11. $\propto$(Fe,Ni) + po
12. $\propto$(Fe,Ni) + γ(Fe,Ni) + po
13. γ(Fe,Ni) + po
14. pn + po + γ(Fe,Ni)
15. pn + γ(Fe,Ni)
16. pn + γ(Fe,Ni) + $FeNi_3$
17. pn + $FeNi_3$
18. pn + $FeNi_3$ + hz
19. pn + hz
20. pn + hz + $\propto Ni_7S_6$
21. pn + $\propto Ni_7S_6$
22. hz + $\propto Ni_7S_6$
23. hz + $FeNi_3$
24. hz + $FeNi_3$ + γ(Fe,Ni)
25. hz + γ(Fe,Ni)
26. po + $(Ni,Fe)_{3\pm x}S_2$ + γ(Fe,Ni)
27. po + $(Ni,Fe)_{3\pm x}S_2$
28. po + $(Ni,Fe)_{3\pm x}S_2$ + pn
29. pn + $(Ni,Fe)_{3\pm x}S_2$
30. pn + $(Ni,Fe)_{3\pm x}S_2$ + Mss
31. $(Ni,Fe)_{3\pm x}S_2$ + Mss
32. $(Ni,Fe)_{3\pm x}S_2$ + γ(Fe,Ni)
33. $(Ni,Fe)_{3\pm x}S_2$ + γ(Fe,Ni) + pn

Symbols

pn = pentlandite = $(Fe,Ni)_9S_8$

po = pyrrhotite = $Fe_{1-x}S$

vs = vaesite = NiS_2

py = pyrite = FeS_2

hz = heazlewoodite = Ni_3S_2

Mss = monosulphide solid solution

$FeNi_3$ = awaruite

(Fe,Ni) = iron-nickel alloy

FeS = troilite

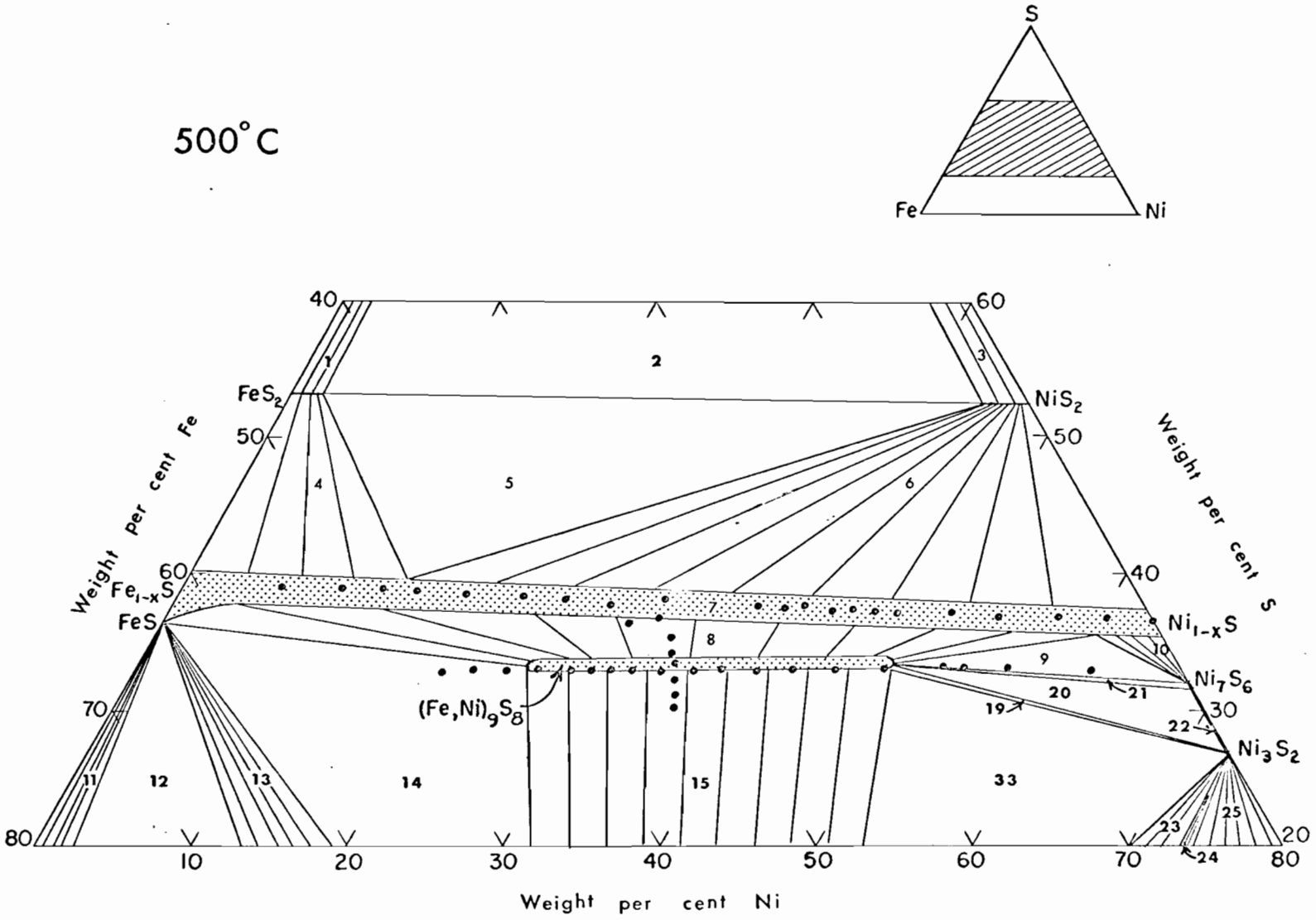

Figure 2. Phase relations in the central portion of the Fe-Ni-S system at 500°C in equilibrium with vapor. Solid circles represent bulk compositions of some runs at 500°C.

Key to Figures 1, 2, and 3

Phases present in equilibrium with vapor

1. py + liquid
2. py + vs + liquid
3. vs + liquid
4. py + Mss
5. py + vs + Mss
6. vs + Mss
7. Mss
8. Mss + pn
9. Mss + pn + $\propto Ni_7S_6$
10. Mss + $\propto Ni_7S_6$
11. $\propto$(Fe,Ni) + po
12. $\propto$(Fe,Ni) + γ(Fe,Ni) + po
13. γ(Fe,Ni) + po
14. pn + po + γ(Fe,Ni)
15. pn + γ(Fe,Ni)
16. pn + γ(Fe,Ni) + $FeNi_3$
17. pn + $FeNi_3$
18. pn + $FeNi_3$ + hz
19. pn + hz
20. pn + hz + $\propto Ni_7S_6$
21. pn + $\propto Ni_7S_6$
22. hz + $\propto Ni_7S_6$
23. hz + $FeNi_3$
24. hz + $FeNi_3$ + γ(Fe,Ni)
25. hz + γ(Fe,Ni)
26. po + $(Ni,Fe)_{3\pm x}S_2$ + γ(Fe,Ni)
27. po + $(Ni,Fe)_{3\pm x}S_2$
28. po + $(Ni,Fe)_{3\pm x}S_2$ + pn
29. pn + $(Ni,Fe)_{3\pm x}S_2$
30. pn + $(Ni,Fe)_{3\pm x}S_2$ + Mss
31. $(Ni,Fe)_{3\pm x}S_2$ + Mss
32. $(Ni,Fe)_{3\pm x}S_2$ + γ(Fe,Ni)
33. $(Ni,Fe)_{3\pm x}S_2$ + γ(Fe,Ni) + pn

Symbols

pn = pentlandite = $(Fe,Ni)_9S_8$

po = pyrrhotite = $Fe_{1-x}S$

vs = vaesite = NiS_2

py = pyrite = FeS_2

hz = heazlewoodite = Ni_3S_2

Mss = monosulphide solid solution

$FeNi_3$ = awaruite

(Fe,Ni) = iron-nickel alloy

FeS = troilite

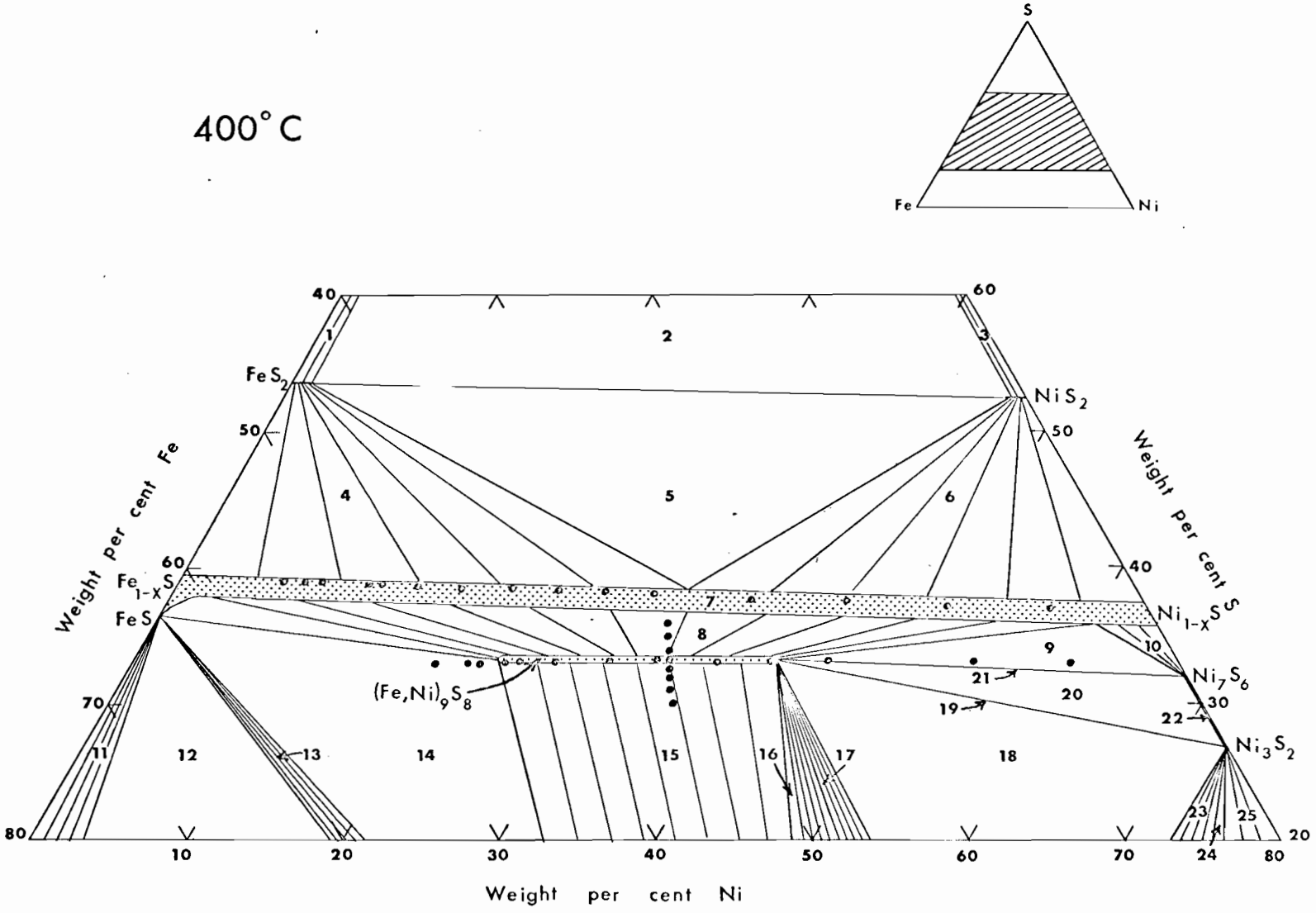

Figure 3 . Phase relations in the central portion of the Fe-Ni-S system at 400°C in equilibrium with vapor. Solid circles represent bulk compositions of some runs at 400°C.

Another major feature of the phase relations shown in Figures 1, 2 and 3 is the presence of extensive iron and nickel solid solution in pentlandite at the 500 and 400°C isotherms. These iron and nickel solid solubility limits are greater than those shown by Kullerud (1963) and Lundqvist (1947). A detailed account of the determination of the solid solubility limits of pentlandite and of the upper stability limit of the pyrite-pentlandite assemblage is given in the following sections.

Solid Solubility Limits of Pentlandite

The solubility limits of pentlandite were determined by silica tube quench experiments at three isotherms, 600, 500 and 400°C. The pentlandite field was studied along two compositional sections at each isotherm; one section at an Fe:Ni atomic ratio of 1:1, and the other section with sulphur constant at about 33.05 weight per cent. The bulk composition of the runs on each isothermal section are shown in Figures 1, 2 and 3. The thermal history of each run and the products formed are shown in Appendix Tables A1 and A2.

X-ray diffraction studies on pentlandite of variable composition show appreciable variation in the 115 spacing. The 115 spacing versus composition diagrams for each isotherm and composition section are shown in Figure 4 and Appendix Figures A1, A2 and A3. An x-ray determinative curve relating d_{115} to the Fe:Ni weight ratio of pentlandite

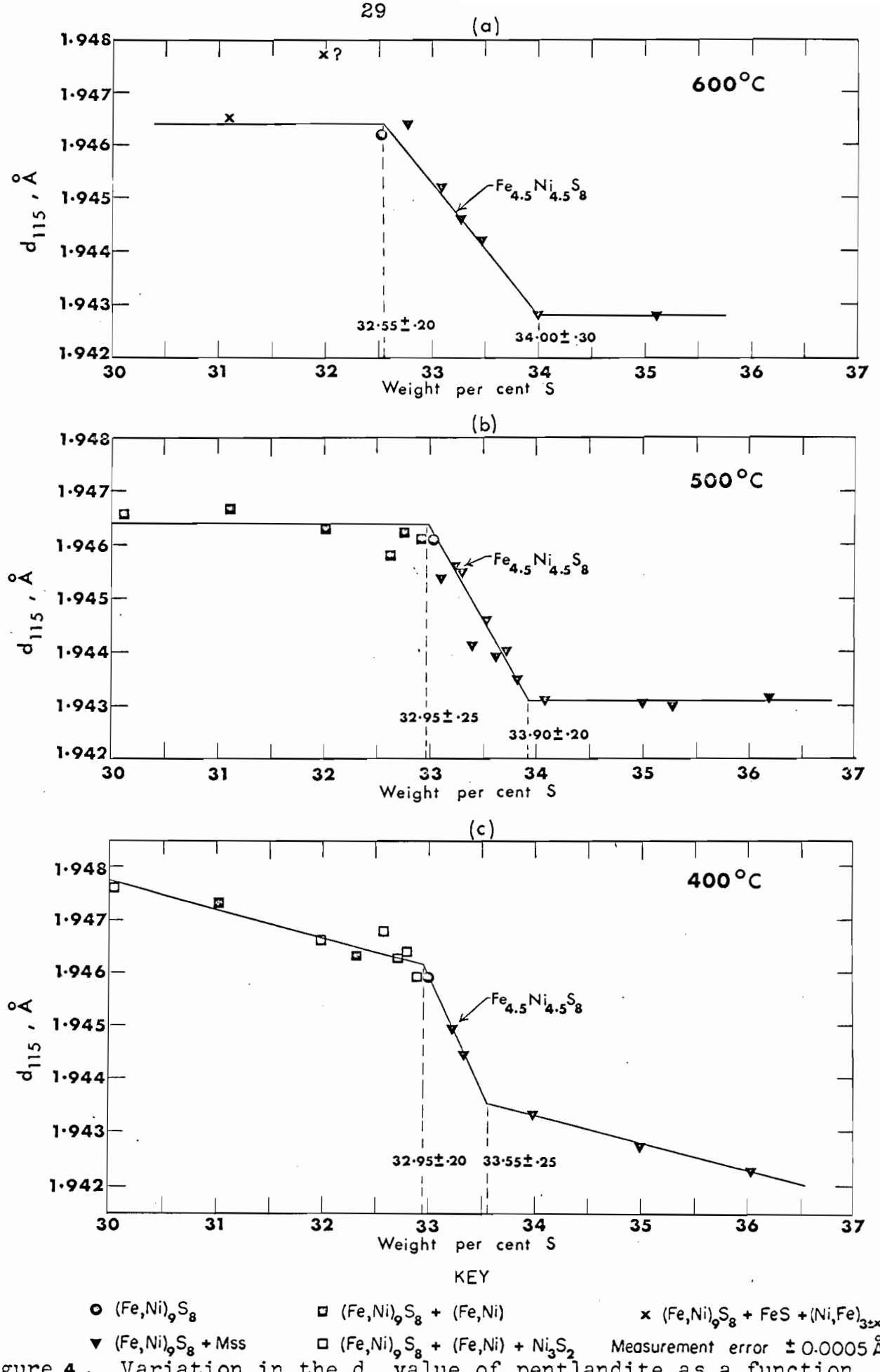

Figure 4. Variation in the d_{115} value of pentlandite as a function of S content along a section Fe : Ni = 1 : 1 (Atomic) at 600, 500, and 400°C. All phases coexist with vapor.

was determined by compiling the data from Appendix Figures A1, A2 and A3 into Figure 5 and is expressed by the equation :

$y = 1.9407 - 0.0023x + 0.0077x^2$, where "y" represents the d_{115} value in Å and "x" represents the iron to nickel weight ratio.

The solubility limit, or phase boundary, of pentlandite is marked by a discontinuity in the d_{115} - composition curve. The accuracy to which the boundary can be determined depends on the precision to which the d - values can be measured and the slope of the d_{115} - composition curve. The accuracy of the boundary determination is not seriously affected by the precision to which the composition is known as the precision in the Fe: Ni ratio is better than 0.008, and the precision in the sulphur content is better than 0.10 mg. The solubility limits of pentlandite as determined from the d_{115} versus composition curves are summarized in Table 2. The data from Table 2 was used to construct the two temperature - composition sections through the pentlandite field shown in Figures 8 and 9. They are described under the heading "Discussion of Results."

As can be seen from the d_{115} - composition curves for the sulphur solubility of pentlandite, Figure 4, runs occurring on the steep sloping portion of the curve are composed of pentlandite plus Mss instead of homogeneous pentlandite as would be expected. The Mss phase occurs as discrete ovoids and clots (Plate 1a) in amounts varying gradationally

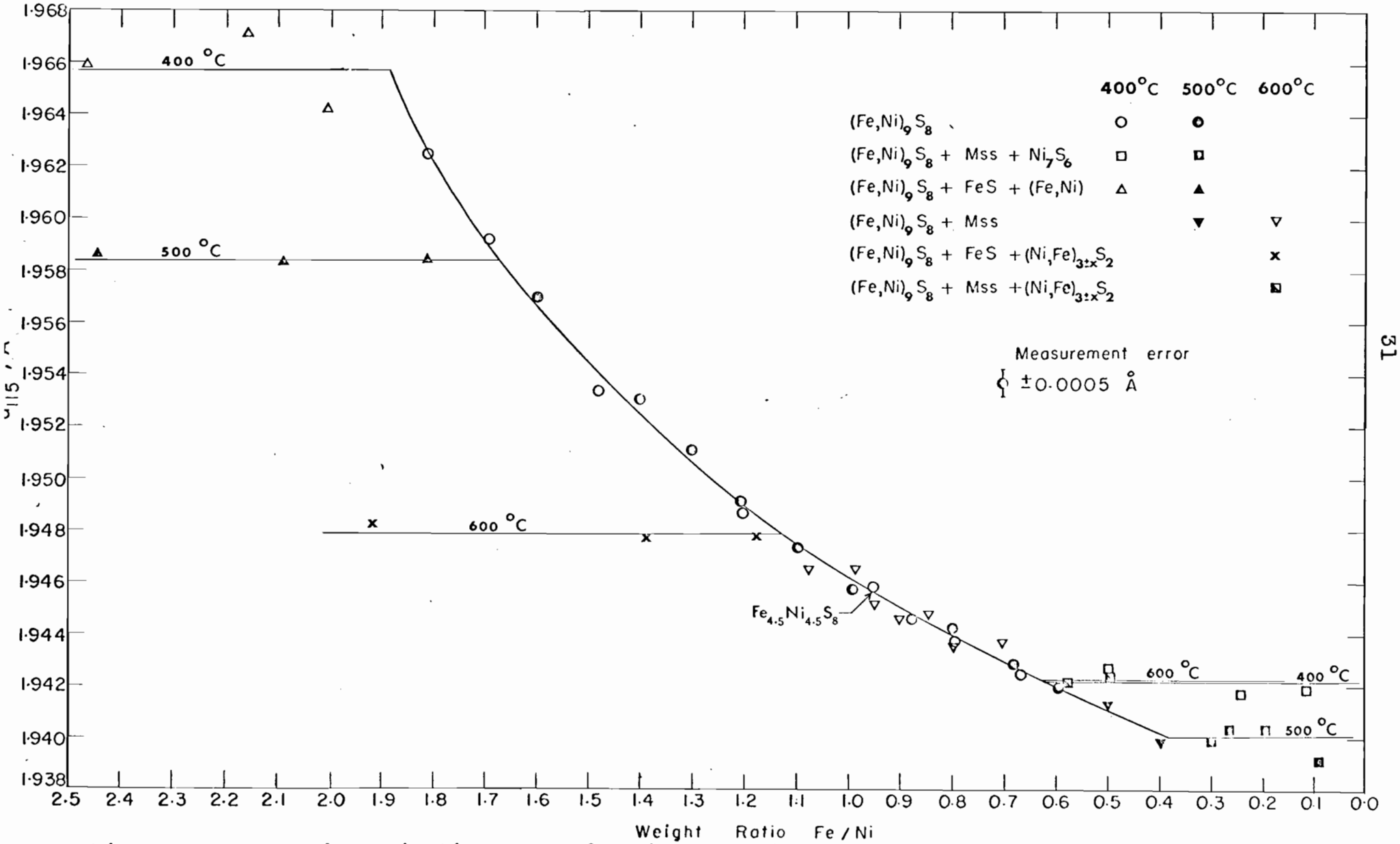

Figure 5. X-ray determinative curve for the Fe : Ni weight ratio of synthetic pentlandite.

TABLE 2

SOLUBILITY LIMITS OF PENTLANDITE DETERMINED FROM d_{115} VERSUS COMPOSITION CURVES

Temperature °C	Sulphur solubility limits at Fe : Ni = 1 : 1 atomic	Iron- and nickel-rich solubility limits with S at 33.05 weight per cent		
	(wt % S)	Fe : Ni weight ratio	wt % Fe	wt % Ni
600	32.55 ± .20 to 34.00 ± .30	1.12 ± .04 0.63 ± .03	35.37 ± .60 25.88 ± .75	31.58 ± .60 41.07 ± .75
500	32.95 ± .25 to 33.90 ± .20	1.67 ± .04 0.38 ± .04	41.88 ± .38 18.44 ± 1.45	25.07 ± .38 48.51 ± 1.45
400	32.95 ± .20 to 33.55 ± .25	1.88 ± .04 0.62 ± .07	43.70 ± .33 25.62 ± 1.77	23.25 ± .33 41.33 ± 1.77

Plate 1a. Ovoids of Mss (light grey) in a predominantly pentlandite (white) charge synthesized at 500°C. Black areas in photomicrographs, unless otherwise stated, are either pits or the plastic cementing medium. Run 66.
Plain, reflected light, 480X.

Plate 1b. Heazlewoodite (dark grey) interstitial to pentlandite (light grey to white) and replacing it along grain boundaries. Synthesized at 600°C. Section stained with dilute chromic acid solution. Run 191.
Plain, reflected light, 480 X.

from about two per cent at the maximum sulphur solubility of pentlandite to nil at the minimum sulphur solubility of pentlandite. A few selected runs occurring on the sloping portion of the curve were heated for periods of about 40 days at 500°C with no apparent change in the abundance of Mss, and no significant change in the d_{115} value of pentlandite. The textural relations between pentlandite and Mss are not suggestive of exsolution phenomena but rather suggest that the Mss phase is present at the temperature of the experiment and is not formed on quenching. If the Mss-pentlandite assemblage represented an equilibrium state, the d_{115} versus composition curve would show an abrupt step-like discontinuity instead of a sloping curve as is the case in the present study. The writer's data suggest that the Mss phase within the pentlandite solid solubility field represents a disequilibrium state in which the amount of Mss is so minute as to have little or no effect on the d_{115} value of pentlandite. Perhaps with a greatly increased heating time the Mss phase would disappear. Further work in this direction is warranted.

Homogeneous pentlandite was successfully synthesized at 500°C and 400°C when the sulphur content of the charge was 33.05 ± .05 weight per cent. Throughout the study on the pentlandite solid solubility field the x-ray powder patterns of homogeneous synthetic pentlandite agreed in general with the latest published powder pattern given for natural pentlandite (Knop and Ibrahim, 1961), with no new reflections or missing

reflections noted. An examination of the d_{115} versus composition curves for the iron- and nickel-rich solubility limits of pentlandite reveals that the d_{115} values change uniformly with composition and that the curves show slight negative deviation from Vegard's law (Vegard's Law: Solid solutions in ionic salts have a linear parameter-composition relationship). The absence of extra reflections in the powder patterns of synthetic pentlandite of various compositions and the uniform parameter-composition curves indicate that the atoms do not form an ordered arrangement (Guinier,1963). The uniform parameter-composition curve would also suggest that defect-type solid solution is absent although density determinations and x-ray intensity measurements would be necessary to substantiate this hypothesis. The results from the writer's study suggest that the solid solution is of the substitutional type, nickel replacing iron atom for atom.

The microscopic appearance and textural relations of synthetic pentlandite and co-existing phases, as determined from polished section studies, did not yield any new information of great significance. Pentlandite of various composition did not show any marked variation in its optical properties; however, on staining with dilute chromic acid, pentlandite was found to exhibit a colour variation from dark golden brown for iron-rich pentlandite to purple for nickel-rich pentlandite. Mss co-existing with pentlandite commonly develops lamellar and network exsolutions of pentlandite in charges quenched from 600 and 500^{o}C (Plate 2), but not in

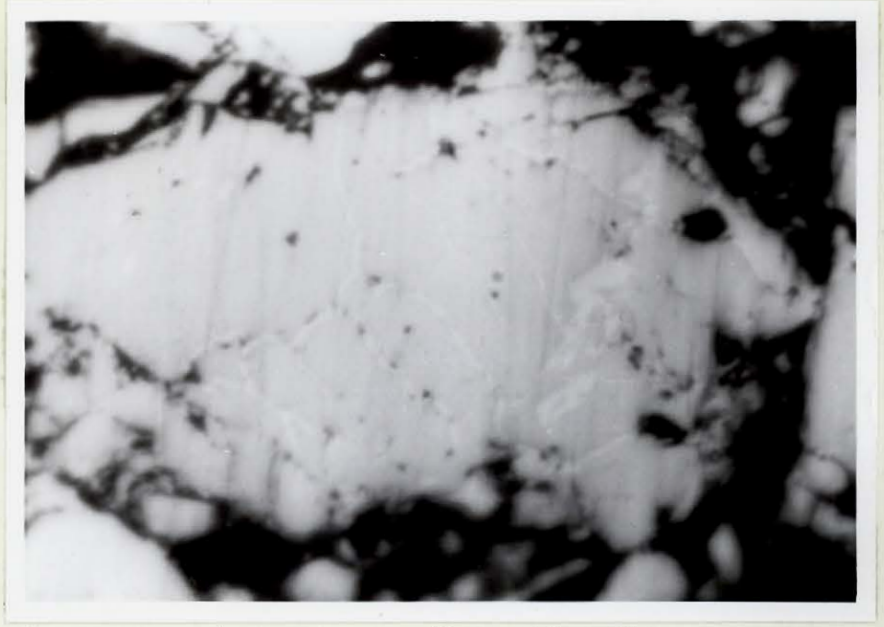

Plate 2a. Fine network texture of pentlandite (white) in Mss (light grey). Synthesized at 600°C. Run 185. Plain, reflected light, 1500 X.

Plate 2b. Pentlandite (light grey) segregations in Mss. Run 185. Plain, reflected light, 480 X.

charges quenched from 400°C. The occurrence of similar textures between natural pentlandite and pyrrhotite is well documented in the literature (Hawley, 1962). The textures observed in the writer's study between synthetic pentlandite and Mss suggest that the natural intergrowths can be formed by a process of exsolution of pentlandite from Mss on cooling. Pentlandite commonly replaces iron-nickel alloy to form much embayed clots and core replacement textures (Plate 3). Heazlewoodite commonly replaces pentlandite along grain boundaries and in places forms core replacement textures (Plate 1b). The textural relationships between primary pentlandite and Mss, and between pentlandite and Ni_7S_6 are not very clear as these assemblages commonly show mutual grain boundary relationships and rarely caries texture.

$Fe_{1-x}S$–$Ni_{1-x}S$ Solid Solution Series

The monosulphide solid solution series was investigated by quench experiments to determine the limits of any solubility gaps and their bearing on the formation of the pyrite-pentlandite tie line. Charges prepared from the elements were made up along a section between $Fe_{0.88}S$ (39.50 wt % S) and $Ni_{0.95}S$ (36.50 wt % S). Initially charges were prepared along this section to fall in the region of about 19 atomic per cent nickel in order that the solubility gap which Kullerud (1963) found at 500 and 400°C could be studied in detail. However, even after

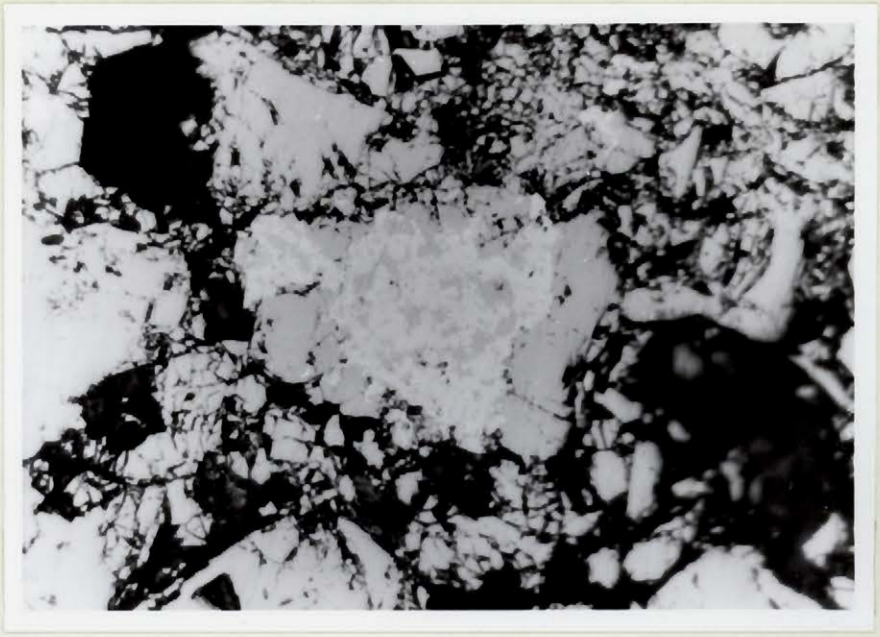

Plate 3a. Iron-nickel alloy (white, centre) replaced by pentlandite (light grey). Synthesized at 400°C. Run 155.
Plain, reflected light, 480 X.

Plate 3b. Irregular clots and "rims" of iron-nickel alloy (white) replaced by pentlandite (light grey). Run 155.
Plain, reflected light, 480 X.

heating charges for periods of up to 35 days at 400°C the x-ray powder patterns and polished sections of the quenched products (Appendix Table A3) from the writer's study indicate that only homogeneous Mss is present at these isotherms where Kullerud showed an immiscibility field. To test the possibility of a solubility gap elsewhere in the section, charges were prepared to cover the entire section at intervals of about 5 atomic per cent nickel. The bulk composition of runs synthesized at 500 and 400°C is shown in Figures 2 and 3. The thermal history and products of these runs is given in Table A3 of the Appendix.

X-ray diffraction studies on Mss of variable composition show appreciable variation in the d_{102} values. The d_{102} values from charges synthesized at 500 and 400°C have been plotted versus composition in Figure 6 and show an interesting anomaly. The d_{102} value of $Fe_{0.88}S$ is decreased linearly by the solution of $Ni_{0.95}S$. At about 29 atomic per cent nickel there is a sudden increase in the rate of decrease of the d_{102} composition curve which terminates at about 33 atomic per cent nickel and a d_{102} value of 2.0106 Å. At this composition a second curve begins with a d_{102} value of 2.0045 Å and maintains a steep slope to about 35 atomic per cent nickel where there is a sudden decrease in slope. From 35 atomic per cent Ni to 48.7 atomic per cent Ni (equivalent to pure $Ni_{0.95}S$) the d_{102} values decrease linearly. The d_{102} values of $Fe_{0.88}S$ (2.0605 Å) and $Ni_{0.95}S$ (1.9840 Å) as determined experimentally

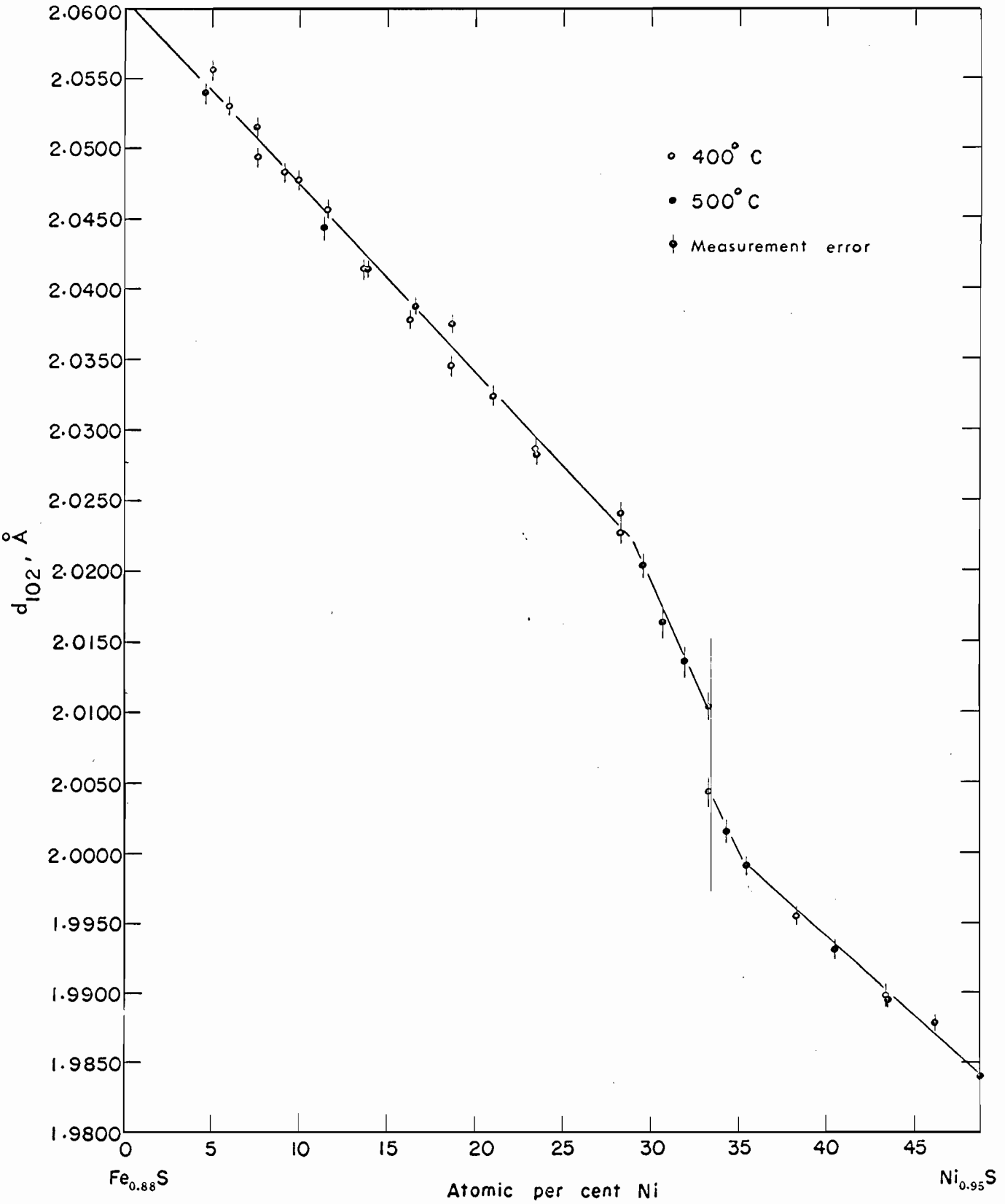

Figure 6. The variation in the d_{102} of the monosulphide solid solution series as a function of nickel content at 500 and 400°C.

in this study or by the projection of the d_{102} - composition curve, agree closely with the published data for pyrrhotite (Arnold, 1962) and $Ni_{1-x}S$ (Arnold and Kullerud, 1956).

An examination of Guinier powder photographs reveals additional characteristics of the monosulphide solid solution series. The pyrrhotite supercell reflections and most of the weak reflections characteristic of pyrrhotite cooled rapidly from above 315°C (Desborough and Carpenter, 1965) are present in Mss from $Fe_{0.88}S$ to about 23 atomic per cent nickel. From 23 atomic per cent nickel to $Ni_{0.95}S$ the Guinier powder photographs display the niccolite-type powder pattern similar to $\propto Ni_{1-x}S$. The x-ray powder patterns also show that the basal reflections undergo the greatest shift with changing composition. Table 3 and Plate 4 illustrate the above changes in the x-ray powder patterns of selected runs across the Mss field.

Two charges (114, 118) occurring at the discontinuity in the d_{102} versus composition curve have anomalous Guinier powder patterns. The 0.0.0.14, 2.0.2.14, 2.0.2.21 and 3.1.4.12 reflections are flanked on either side by slightly diffuse, but well-resolved, satellites or side-bands (see Plate 4b). The other reflections have very weak and diffuse side-bands that were too poorly resolved to be measured and shown in Table 3. This phenomenon has been called a modulated structure (Taylor, 1961) and was first discovered by Bradley (1940) in a study of alloys centered

TABLE 3

SELECTED MONOSULPHIDE SOLID SOLUTION X-RAY DATA FROM GUINIER POWDER PHOTOGRAPHS USING Co $K\alpha_1$ RADIATION COMPARED TO DESBOROUGH AND CARPENTER'S (1965) DATA FOR PYRRHOTITE

Films corrected for shrinkage using Si(a = 5.428Å) as internal standard.

					$Fe_{1-x}S$ 47.5 A.% Fe (1) Desborough & Carpenter (1965)	Run 110 (2) $Fe_{0.68}Ni_{0.22}S$ (11.35 At.% Ni)	Run 172 (2) $Fe_{0.36}Ni_{0.57}S$ (29.53 At.% Ni)	Run 114 (2) $Fe_{0.29}Ni_{0.64}S$ (33.16 At.% Ni)	Run 116 (2) $Fe_{0.10}Ni_{0.84}S$ (43.48 At.% Ni)
h	k	i	l	Rel. Int.	d(obs)Å	d(obs)Å	d(obs)Å	d(obs)Å	d(obs)Å
1	0	$\bar{1}$	2	mw	5.72	5.71	n.o.	n.o.	n.o.
1	0	$\bar{1}$	4	vvw	5.16	5.56	n.o.	n.o.	n.o.
1	0	$\bar{1}$	5	vvw	4.76	4.74	n.o.	n.o.	n.o.
1	0	$\bar{1}$	6	vvw	4.39	4.05	n.o.	n.o.	3.95
1	1	$\bar{2}$	2	vvw	3.40	3.41	n.o.	n.o.	n.o.
2	0	$\bar{2}$	0	s	2.982	2.970	2.973	2.970 2.769*	2.966
0	0	0	14	w	2.861	2.818	2.765	2.738 2.701*	2.677
2	0	$\bar{2}$	7	s	2.647	2.629	2.617	2.614	2.599
1	1	$\bar{2}$	11	vvw	2.473	n.o.	n.o.	n.o.	n.o.
1	1	$\bar{2}$	12	vw	2.394	2.408	n.o.	n.o.	n.o.
2	1	$\bar{3}$	2	vvw	2.241	n.o.	n.o.	n.o.	n.o.
2	1	$\bar{3}$	5	vw	2.165	2.154	n.o.	n.o. 2.024*	n.o.
2	0	$\bar{2}$	14	vs	2.067	2.040	2.019	2.013 1.999*	2.405

Continued

TABLE 3

2	1	$\bar{3}$	9	vvw	2.017	n.o.	n.o.	n.o.	n.o.
3	0	$\bar{3}$	2	vvw	1.981	1.973	n.o.	n.o.	n.o.
3	0	$\bar{3}$	5	vvw	1.927	n.o.	n.o.	n.o.	n.o.
1	1	$\bar{2}$	18)	vvw	1.866	n.o.	n.o.	n.o.	n.o.
2	1	$\bar{3}$	12)						
3	0	$\bar{3}$	9	vw	1.818	1.789	n.o.	n.o.	n.o.
3	0	$\bar{3}$	11	vvw	1.746	n.o.	n.o.	n.o.	n.o.
2	2	$\bar{4}$	0	s	1.721	1.713	1.714	1.713 1.573*	1.714
2	0	$\bar{2}$	21	m	1.609	1.586	1.562	1.563 1.554*	1.528
4	0	$\bar{4}$	0	mw	1.492	1.486	1.486	1.485	1.486
3	1	$\bar{4}$	12	vvw	1.477	1.463	1.457	1.453	1.445
4	0	$\bar{4}$	7	m	1.444	1.436	1.434	1.434	1.431
0	0	0	28	m	1.434	1.406	1.371	n.o.	n.o.

plus additional lines, not measured

---

n.o. not observed

* DIFFUSE SIDE-BANDS

(1) Synthesized at 650°C, annealed at 420°C for 24 hrs. and quenched

(2) Annealed at 500°C for about 20 days and quenched

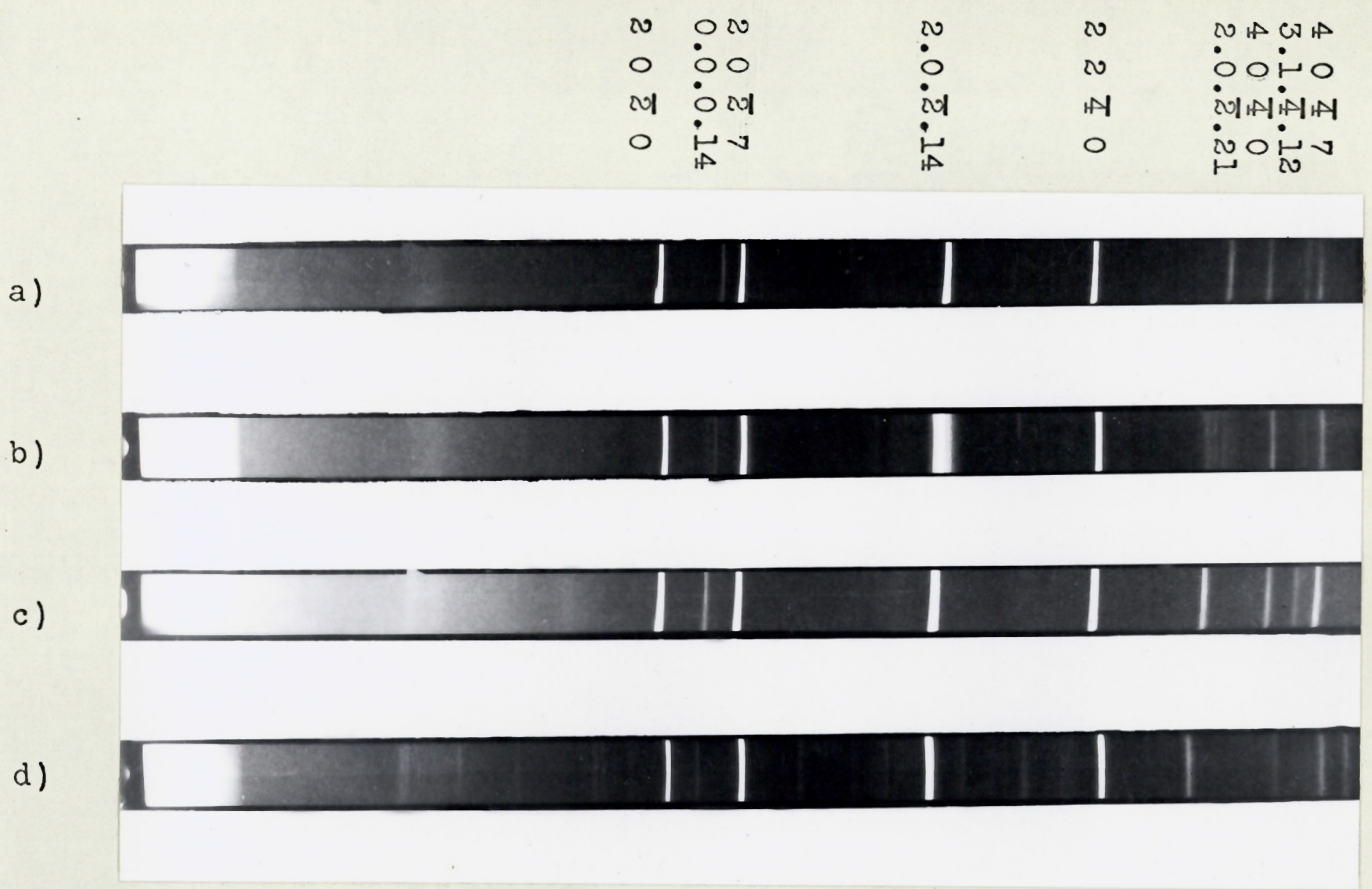

Plate 4 . Selected Guinier powder photographs of monosulphide solid solution synthesized at 500°C and quenched. Co α_1 radiation. Indices are shown for some of the prominent reflections.

a) Run 116, $Fe_{0.10}Ni_{0.84}S$, 43.48 at. % Ni, NiAs structure.

b) Run 114, $Fe_{0.29}Ni_{0.64}S$, 33.16 at. % Ni, modulated structure.

c) Run 112, $Fe_{0.38}Ni_{0.54}S$, 28.19 at. % Ni, NiAs structure.

d) Run 113, $Fe_{0.75}Ni_{0.14}S$, 7.62 at. % Ni, note weak additional reflections characteristic of pyrrhotite.

around the composition of Cu_4FeNi_3 of the Cu - Fe - Ni system. In the case of the Cu_4FeNi_3 alloy, the structure is produced when a homogeneous face-centered cubic phase separates below a certain temperature into two cubic phases of different composition, but with nearly equal lattice parameters. If the homogeneous solid solution is equilibrated at successively lower temperatures, several intermediate stages are observed, the first of which is characterized by powder patterns showing the diffraction lines for a single cubic phase, each line being flanked by weak and diffuse side-bands. Clearly then, the modulated structure in Mss at 33 atomic per cent nickel represents the composition at which Mss begins to break down into two Mss phases of different composition. The steep portions of the d_{102} - composition curves occurring on either side of the discontinuity must be related in some way to this modulated structure. A thorough crystallographic investigation of the Mss field would be necessary for a more complete interpretation of the anomalous d_{102} - composition curves, but this is beyond the scope of the present investigation.

Colgrove (1942) noted a sudden change in the axial ratio of Mss between Fe:Ni molar ratios of 1:0.73 and 1:1.0. In the writer's study, the modulated structure occurs at a molar ratio of 0.45. This discrepancy cannot be completely resolved with the present data; however, since Colgrove slowly cooled his runs, it is suggested that he may have taken

some crystallographic measurements on heterogeneous Mss mixtures. It is also apparent from Colgrove's experimental data that some of his "Mss" charges contained minor amounts vaesite and/or pentlandite; thus either equilibrium was not attained or the bulk composition of his runs were not as well known as believed.

Since a solubility gap in the Mss field was not found at 500 and 400°C, selected charges were subsequently annealed at 350, 300 and 200°C for periods of about 40 days. The quench products from runs at 350 and 300°C were found to contain only homogeneous Mss. However, the Mss annealed at 200°C had broken down into two Mss phases plus about 10 per cent pentlandite. The composition of the two coexisting Mss phases was determined by measuring the d - values of the 102 reflections, and by using the d_{102} - composition curve (Figure 6) as a determinative curve. The results of these observations are shown in Table 4.

As can be seen from Table 4, an extensive immiscibility field, exists along the $Fe_{0.88}S$ to $Ni_{0.95}S$ section at 200°C from about 12 to 31 atomic per cent Ni. Theoretically the pyrite-pentlandite tie line should intersect the Mss section at about 19 atomic per cent Ni, well within the immiscibility field at 200°C. From a consideration of the bulk composition of the Mss charges, the products formed on annealing at 200°C, and the geometry of the phase diagram, the assemblage Mss_1 plus Mss_2 plus pentlandite is thought to represent a non-equilibrium assemblage. Pyrite

TABLE 4

RESULTS OF ANNEALING HOMOGENEOUS MONOSULPHIDE SOLID SOLUTIONS ALONG THE $Fe_{0.88}S$ TO $Ni_{0.95}S$ SECTION AT $200^{\circ}C$ FOR 40 DAYS

Run	Atomic % Ni	Products Compositions in parenthesis are atomic % Ni
109	4.55	Homogeneous Mss
117	4.97	Homogeneous Mss
98	13.70	Mss_1 (31) plus Mss_2 (12) plus pn
94	13.79	Mss_1 (31) plus Mss_2 (14) plus pn
101	16.25	Mss_1 (31) plus Mss_2 (12) plus pn
104	20.89	Mss_1 (31) plus Mss_2 (10) plus pn
96	23.44	Mss_1 (39) plus Mss_2 (24) plus pn
112	28.19	Mss_1 (30) plus Mss_2 (?) plus pn

should be part of this assemblage if equilibrium was attained. The lack of pyrite in the runs examined probably is due to a problem of nucleation. Although the Mss_1-Mss_2- pentlandite assemblage represents non-equilibrium, the results suggest that the pyrite-pentlandite tie line forms at some temperature between 300 and 200°C. The data shown in Figure 6 and in Table 4 has been used to construct a generalized, semi-schematic temperature — composition section along an $Fe_{1-x}S$ - $Ni_{1-x}S$ join. This diagram is shown in Figure 11 and described under the heading "Discussion of Results."

Upper Stability Limit of the Pyrite-Pentlandite Assemblage

The upper stability limit of the pyrite-pentlandite assemblage was investigated by studying the reaction pyrite + pentlandite $\rightleftharpoons$Mss at various temperatures. Previously synthesized pyrite and pentlandite were mixed together to form a charge with a bulk composition of 36.17 weight per cent Fe, 25.60 weight per cent Ni, and 38.23 weight per cent S. The pentlandite used to make up this charge was not homogeneous but contained less than one per cent Mss. This Mss could readily be distinguished when the charge was equilibrated at successively lower temperatures as it exsolved pentlandite to form the characteristic lamellar and network exsolution textures. The reverse reaction Mss$\rightarrow$pyrite pentlandite was studied by annealing previously synthesized Mss of composition 36.20 weight per cent Fe, 25.40 weight per cent Ni, and

38.40 weight per cent S, at various temperatures. The charges were loaded into silica glass tubes, glass rods inserted to keep the vapor volume to a minimum, and heated at various temperatures. The runs were periodically examined with polished sections and the Guinier x-ray camera to determine to what degree the reaction had proceeded. The results of these observations are shown in Table 5.

As can be seen from Table 5, the pyrite and pentlandite charges reacted rapidly to form Mss above 300°C. As can be seen in Figure 7 the rate of reaction below 300°C was quite sluggish and the amount of Mss formed very minor. The Mss formed in the runs below 300°C developed as core replacement of both pentlandite and pyrite, and as a narrow reaction rim around the pyrite grains (Plate 5). The results of this study suggest that the pyrite-pentlandite assemblage becomes stable at some temperature below 260°C.

The results of experiments on the reverse reaction were inconclusive. Mss was found to break down into two Mss phases at 270°C but not at 280°C. The two Mss phases form a characteristic emulsion exsolution texture. Mss annealed at 200°C for 24 days exsolved about 10 per cent pentlandite in the characteristic net texture. No further significant change in the amount of pentlandite formed was observed even after heating at 200°C for 66 days. At no stage in the experiments was pyrite seen to form as a result of Mss breakdown. If the reaction had

TABLE 5

DETERMINATION OF THE UPPER STABILITY OF THE PYRITE-PENTLANDITE ASSEMBLAGE

Starting Material	T (°C)	Time (days)	Products
(a) The reaction py + pn ⟶ Mss			
py + pn	500	22.0	Mss
py + pn	450	22.0	Mss
py + pn	400	22.0	Mss
py + pn	350	15.0	Mss + minor py and pn
py + pn	300	15.0	py + pn + minor Mss
py + pn	290	15.0	py + pn + minor Mss
py + pn	290	34.8	py + pn + minor Mss
py + pn	280	15.0	py + pn + very minor Mss
py + pn	280	34.8	py + pn + minor Mss
py + pn	270	15.0	py + pn
py + pn	270	35.6	py + pn + very minor Mss
py + pn	260	15.0	py + pn
py + pn	260	33.6	py + pn
py + pn	250	15.0	py + pn
py + pn	250	48.0	py + pn
(b) The reaction Mss ⟶ py + pn			
Mss	500	25.0	Mss
Mss	450	25.0	Mss
Mss	400	25.0	Mss
Mss	350	16.8	Mss
Mss	300	16.8	Mss
Mss	290	14.5	Mss
Mss	290	33.7	Mss
Mss	280	14.5	Mss
Mss	280	33.7	Mss
Mss	270	14.5	Mss
Mss	270	35.4	Mss_1 + Mss_2
Mss	260	33.6	Mss_1 + Mss_2
Mss	250	15.1	Mss_1 + Mss_2
Mss	250	48.1	Mss_1 (31 at % Ni) + Mss_2 (19 at % Ni)
Mss	200	24.8	Mss_1 + Mss_2 + pn
Mss	200	66.3	Mss_1 (33 at % Ni) + Mss_2 (14 at % Ni) + pn

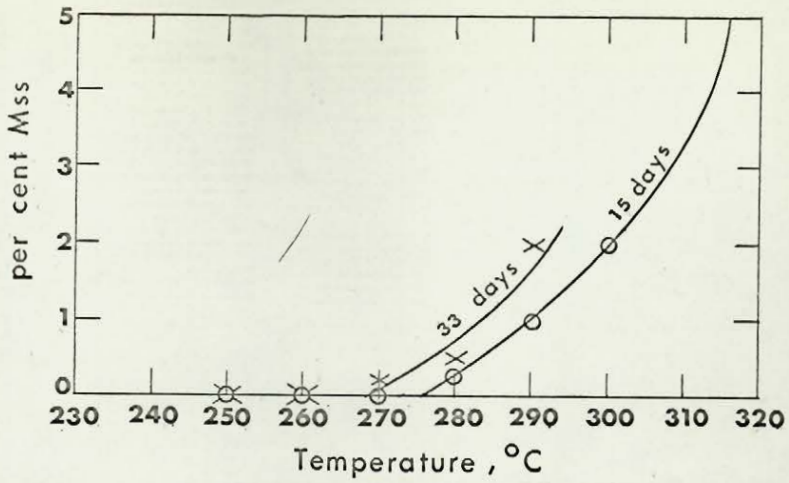

Figure 7. Rate of formation of Mss from pyrite-pentlandite charges.

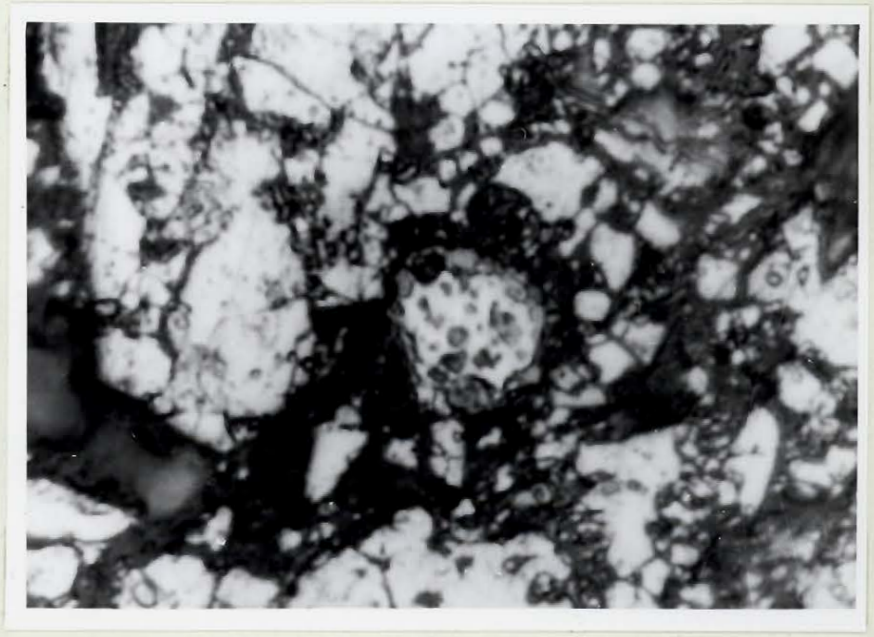

Plate 5. Pyrite (white, centre) corroded and rimmed by Mss (intermediate grey) at 280°C. Pentlandite (light grey). Section stained with dilute chromic acid solution.
Plain, reflected light, 1500 X.

proceeded to completion the products would consist of about 75 per cent pentlandite and 25 per cent pyrite. In the experiments at 200°C only about 13 per cent of the required amount of pentlandite had formed when Mss was heated for 66 days. From a consideration of the bulk composition of the Mss charge and the geometry of the phase diagram, the assemblage Mss_1 plus Mss_2 plus pentlandite is interpreted to represent a non-equilibrium assemblage. It appears that the reaction rate of Mss breakdown is too sluggish for an effective determination of the temperature at the invariant point.

As the invariant point for the assemblage pyrite plus pentlandite plus Mss_1 plus Mss_2 plus vapor can only be determined with a reasonable degree of confidence when the reaction is studied from both directions, the conclusions from the writer's results can only be tentative until additional experiments are performed. However, the results of annealing Mss of various compositions at 200°C (Table 4) suggest that the pyrite-pentlandite tie line forms at some temperature above 200°C, thus the upper stability limit of the pyrite-pentlandite assemblage is stated as 230 ± 30°C. A suggested method for more closely defining the invariant point is to study the reaction pyrrhotite + millerite $\rightleftharpoons$ pyrite + pentlandite, or to seed Mss charges with minor amounts of pyrite to promote nucleation.

High Temperature X-ray Powder Diffraction

A Rigaku-Denki high temperature x-ray powder diffraction camera was used to determine the approximate breakdown temperature of synthetic pentlandite, and the non-quenchable high temperature products of this breakdown. For this experiment pentlandite of composition 32.64 weight per cent Fe, 34.31 weight per cent Ni, and 33.05 weight per cent S was synthesized at 580°C and rapidly quenched. The pentlandite was not homogeneous but contained about one half per cent Mss. This minor impurity did not adversely affect the results of the experiment. Using Fe radiation, the following exposure sequence was followed: 25°C, 200°C, 300°C, 500°C, 665°C and 25°C. All exposures, except the 665°C exposure, showed the pentlandite x-ray pattern. The 665°C exposure was repeated using Cu radiation, the results of which are compared to those of Kullerud (1963) in Table 6.

As can be seen from Table 6 the writer's results agree closely with those of Kullerud. Kullerud showed that five of the reflections closely coincide with those of hexagonal pyrrhotite and the remaining four belong to the nonquenchable $(Ni, Fe)_{3\pm x}S_2$ phase. Kullerud (1963) was able to show by D. T. A. experiments that the invariant temperature for pentlandite decomposition is 610 ± 2°C.

Discussion of Results

The phase relations found in the writer's study (Figures 1, 2

TABLE 6

COMPARISON OF THE HIGH TEMPERATURE X-RAY POWDER DIFFRACTION DATA ON THE BREAKDOWN PRODUCTS OF PENTLANDITE
(Ni-filtered Cu radiation)

Kullerud (1963)		This study		Berry & Thompson (1962)		Killerud & Yund (1962)	
$Fe_{4.5}Ni_{4.5}S_8$ 670°C		$Fe_{4.5}Ni_{4.5}S_{7.9}$ 665°C		Natural Hexagonal Pyrrhotite Room Temperature		$Ni_{3-x}S_2$ 650°C	
I	d in Å	I	d in Å	I	d in Å	I	d in Å
w	3.038	vvw	3.382	4	3.00		
m	2.950	m	2.999			100	2.96
w	2.662	m	2.657	6	2.65		
m	2.078	s	2.061	10	2.08		
s	1.835	ms	1.825			100	1.823
w	1.758	m	1.744	5	1.728		
vw	1.567	vvw	1.598			50	1.511
vw	1.345	vw	1.335	4	1.328		
vw	1.297		n.o.			20	1.289

n.o. not observed

and 3) indicate some changes in the phase diagrams of Kullerud (1963). The major differences found at the isothermal sections studied are:

1) a more extensive field of iron and nickel solid solubility in pentlandite,

2) a continuous monosulphide solid solution series, and

3) a tie line between $Ni_7 S_6$ and pentlandite at 500 and 400°C.

The pyrite-pentlandite stability study indicates that the pyrite-pentlandite tie line forms at 230 ± 30°C instead of 450°C as Kullerud reported. The above differences suggest that some of Kullerud's interpretation of the ternary phase relations in the metal-rich portion of the Fe-Ni-S system was in error in many respects and that further research into the Fe-Ni-S system may well yield new data of interest to geologists.

Data from the present study has been incorporated with Kullerud's findings to produce two temperature - composition sections through the pentlandite field. Since the sections are not binary in nature, they cut through some ternary univariant fields. The vertical section (Figure 8) drawn at an Fe : Ni atomic ratio of 1 : 1 shows that the solubility of sulphur in pentlandite is a function of temperature reaching both minimum (33.5 wt % S) and maximum (34.1 wt % S) values at about 580°C. This confirms Kullerud's (1963) suggestion that the maximum metal to sulphur ratio is reached at about 580°C when, on cooling, the assemblage pentlandite plus γ(Fe,Ni) alloy becomes stable. The shape of the pentlandite

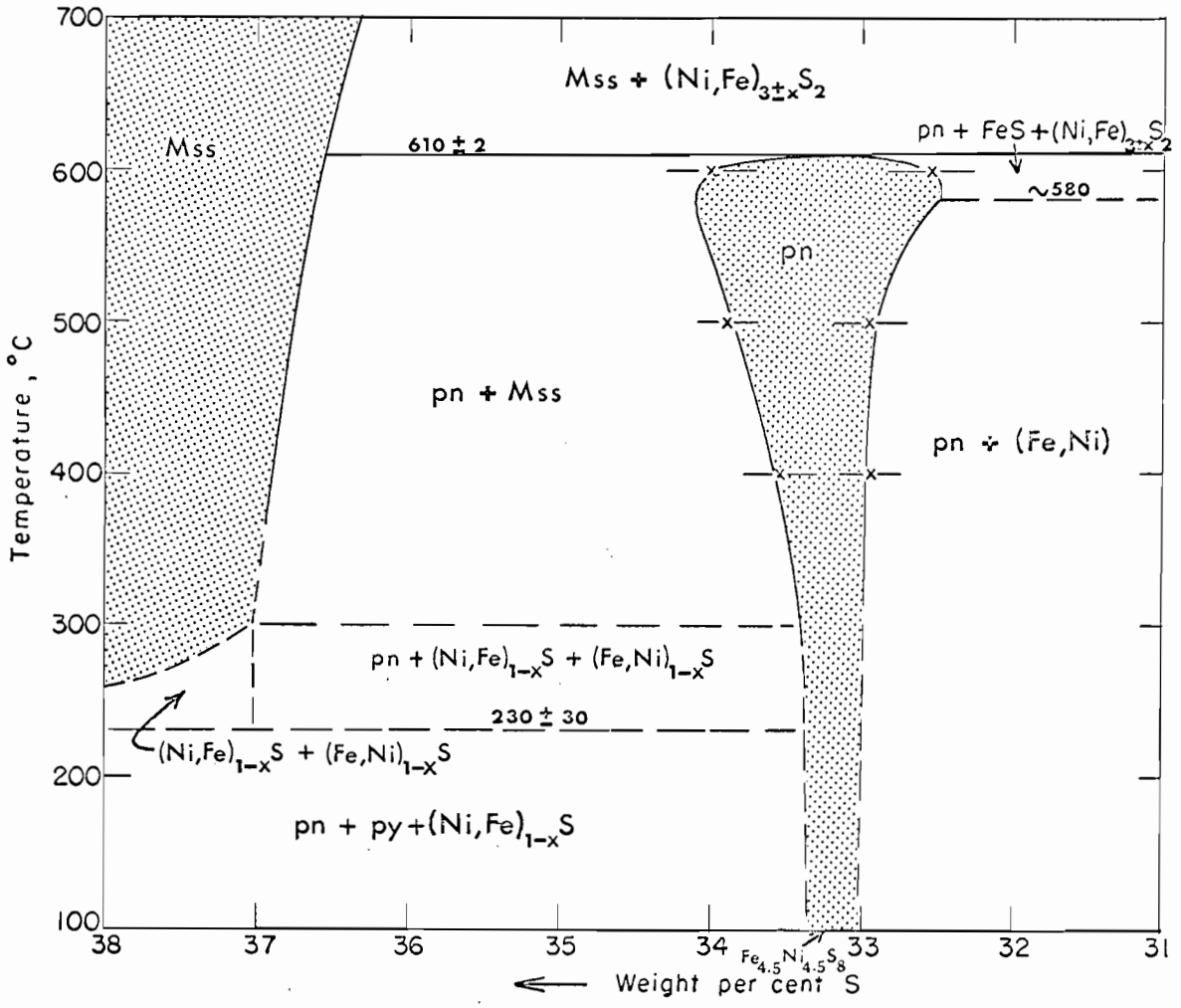

Figure 8. Phase relations in the central portion of the Fe-Ni-S system along a section through Fe : Ni = 1 : 1 (Atomic). A portion of the Mss solvus is from Kullerud (1956) and dashed portions are only approximate.

solvus towards the Mss field supports Hawley's (1962) suggestion that some natural pyrrhotite included within pentlandite may result from the exsolution of pyrrhotite from a sulphur-rich pentlandite on slow cooling.

As can be seen from Figure 9, the iron and nickel solid solubility field of pentlandite has a rather odd shape; with a maximum nickel solubility at about 500°C of approximately 48 weight per cent nickel, and some suggestion that the pentlandite field narrows considerably at lower temperatures. Additional experiments below 400°C to determine the extent of the apparent narrowing of the pentlandite field is warranted as this may well explain the limited range in composition of natural pentlandites from many ore bodies.

The writer's results are combined with those of Kullerud (1963) and Lundqvist (1947) in Figure 10 to show the phase relations of the Fe-Ni-S system at 200°C. All of Kullerud's (1963) phase relations for the portion of the system more sulphur-rich than Fe S — Ni S were taken from Clark and Kullerud (1963). The phase relations below 400°C on the Fe — Ni binary section are imperfectly known and have been approximated in the construction of Figure 10 by extrapolation to 200°C of data presented in Hansen and Anderko (1958) and Elliott (1965). The ternary phase relations must be considered tentative as they are based on a small number of experimental runs, which in many cases failed to reach equilibrium. The exact position of the boundaries between the two-

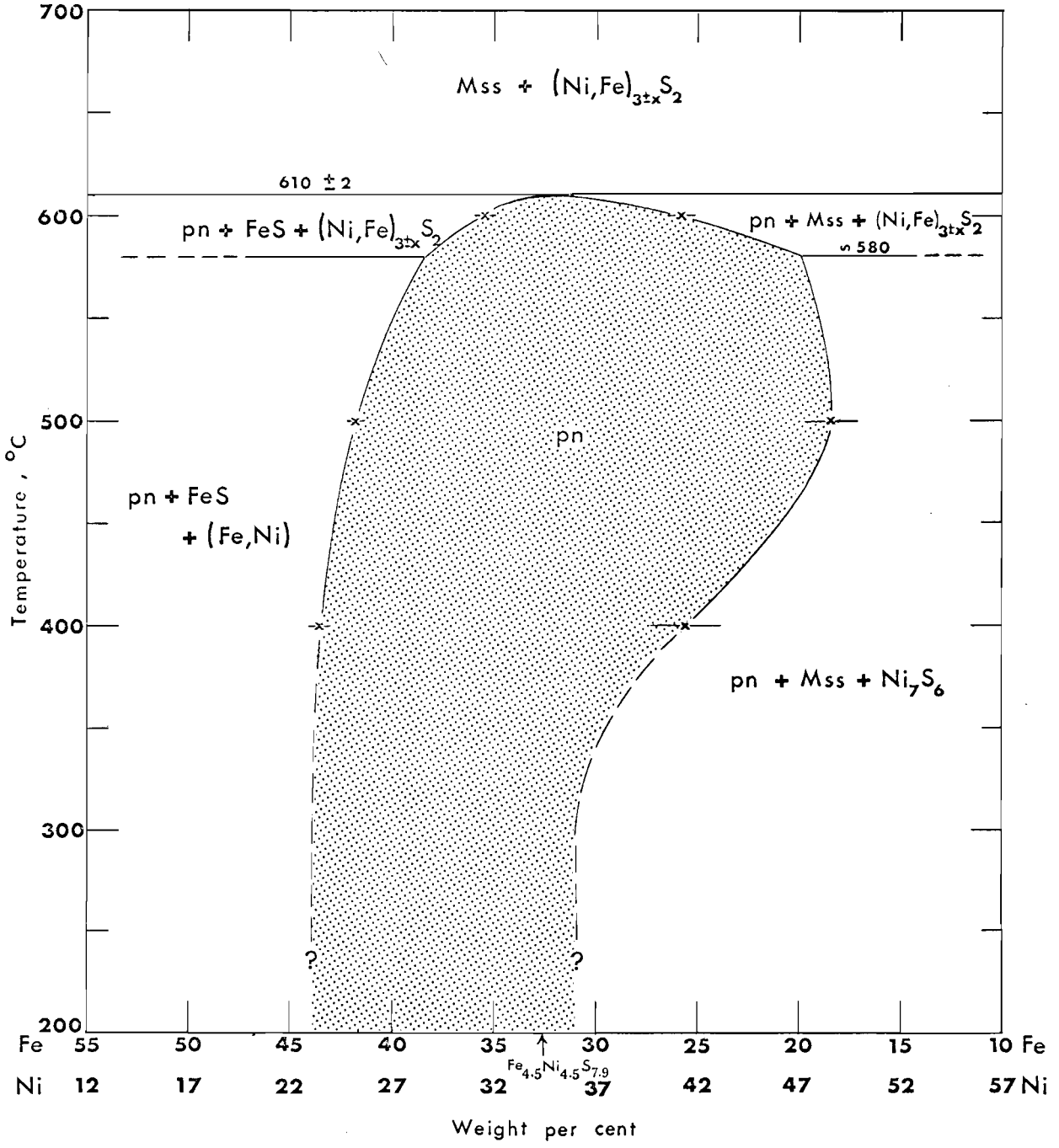

Figure 9 . Vertical section through the pentlandite solid solution field at 33 weight per cent sulphur.

Key to Figure 10

Phases present in equilibrium with vapor

1. py + liquid
2. py + vs + liquid
3. vs + liquid
4. py + vs
5. Mss + po + Fe_7S_8
6. Mss + py + Fe_7S_8
7. Mss + py
8. Mss + py + pn
9. py + pn
10. py + pn + vl
11. py + vl
12. py + vl + vs
13. vl + vs
14. vl + vs + pm
15. vl + pm
16. vl + pm + Mss
17. vl + Mss
18. vl + Mss + pn
19. vl + pn
20. Mss + pn
21. Mss
22. Mss + pm
23. Mss + pm + ml
24. Mss + ml
25. Mss + ml + pn
26. pn + ml
27. pn + ml + βNi_7S_6
28. pn + βNi_7S_6
29. pn + βNi_7S_6 + hz
30. pn + hz
31. hz + γ(Fe,Ni)
32. hz + γ(Fe,Ni) + $FeNi_3$
33. hz + $FeNi_3$
34. hz + $FeNi_3$ + pn
35. pn + $FeNi_3$
36. pn + $FeNi_3$ + γ(Fe,Ni)
37. pn + γ(Fe,Ni)
38. po + γ(Fe,Ni)
39. po + γ(Fe,Ni) + α(Fe,Ni)
40. po + α(Fe,Ni)
41. Mss + pn
42. Mss
43. pn + po + γ(Fe,Ni)

Symbols

pn = pentlandite = $(Fe,Ni)_9S_8$

po = pyrrhotite = $Fe_{1-x}S$

ml = millerite = $Ni_{1-x}S$

py = pyrite = FeS_2

vs = vaesite = NiS_2

hz = heazlewoodite = Ni_3S_2

pm = polydymite = Ni_3S_4

vl = violarite = $(Ni,Fe)_3S_4$

Mss = monosulphide solid solution

$FeNi_3$ = awaruite

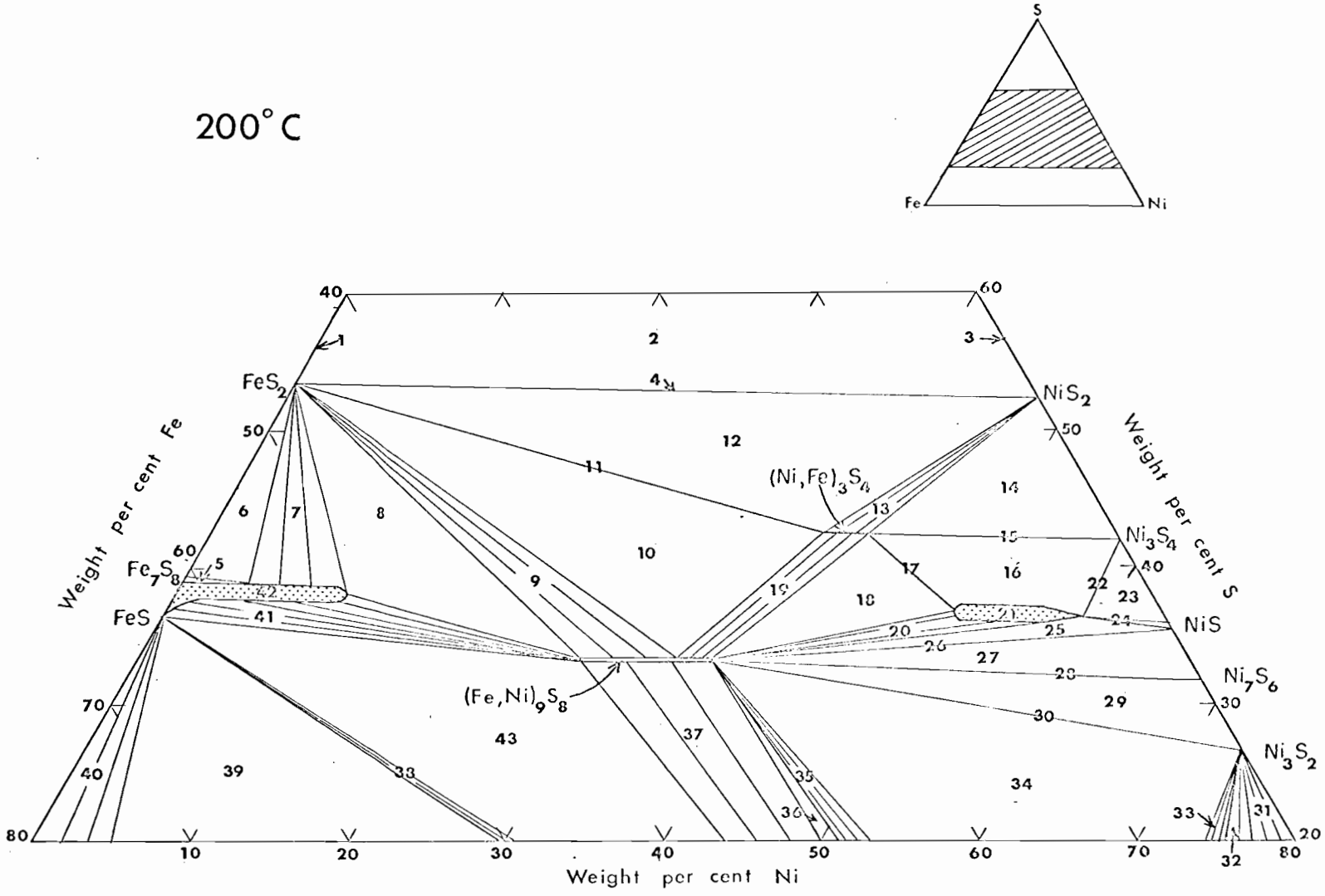

Figure 10. Approximate phase relations in the central portion of the Fe-Ni-S system at 200°C in equilibrium with vapor.

and three - phase regions is uncertain and the presence of tie lines between two phases is in some cases inferred. As can be seen from Figure 10 an extensive immiscibility field extends between $(Fe, Ni)_{1-x}S$ and $(Ni, Fe)_{1-x}S$ permitting tie lines to form between pyrite and pentlandite, and violarite and pentlandite. As millerite is the stable form of Ni S below 396°C (Kullerud and Yund, 1962), the $(Ni, Fe)_{1-x}S$ phase becomes separated from millerite by the divariant field $(Ni, Fe)_{1-x}S$ plus Ni S. The $Ni_3 S_4$ phase, polydymite, is stable below 356 ± 3°C (Kullerud and Yund). The upper stability limit and composition limits of $(Ni, Fe)_3 S_4$, violarite, are unknown but Lundqvist found $Ni_2 Fe S_4$ to be present at 200°C. In Figure 10 the composition limits of violarite and polydymite are assumed to be narrow. The pentlandite field is inferred to have narrowed considerably from the extensive iron and nickel solid solubility limits shown at 400°C.

The results of investigations into the monosulphide solid solution series and into the upper stability limit of the pyrite - pentlandite assemblage are incorporated in a generalized, semi-schematic section along an $Fe_{1-x}S$ — $Ni_{1-x}S$ join shown in Figure 11. This diagram, while being tentative and approximate in many places, helps to clarify the writer's observations along this section. Since the section is not a true binary section, the phase relations are very complex. The complexity of this section is in part due to the complex nature of the end members

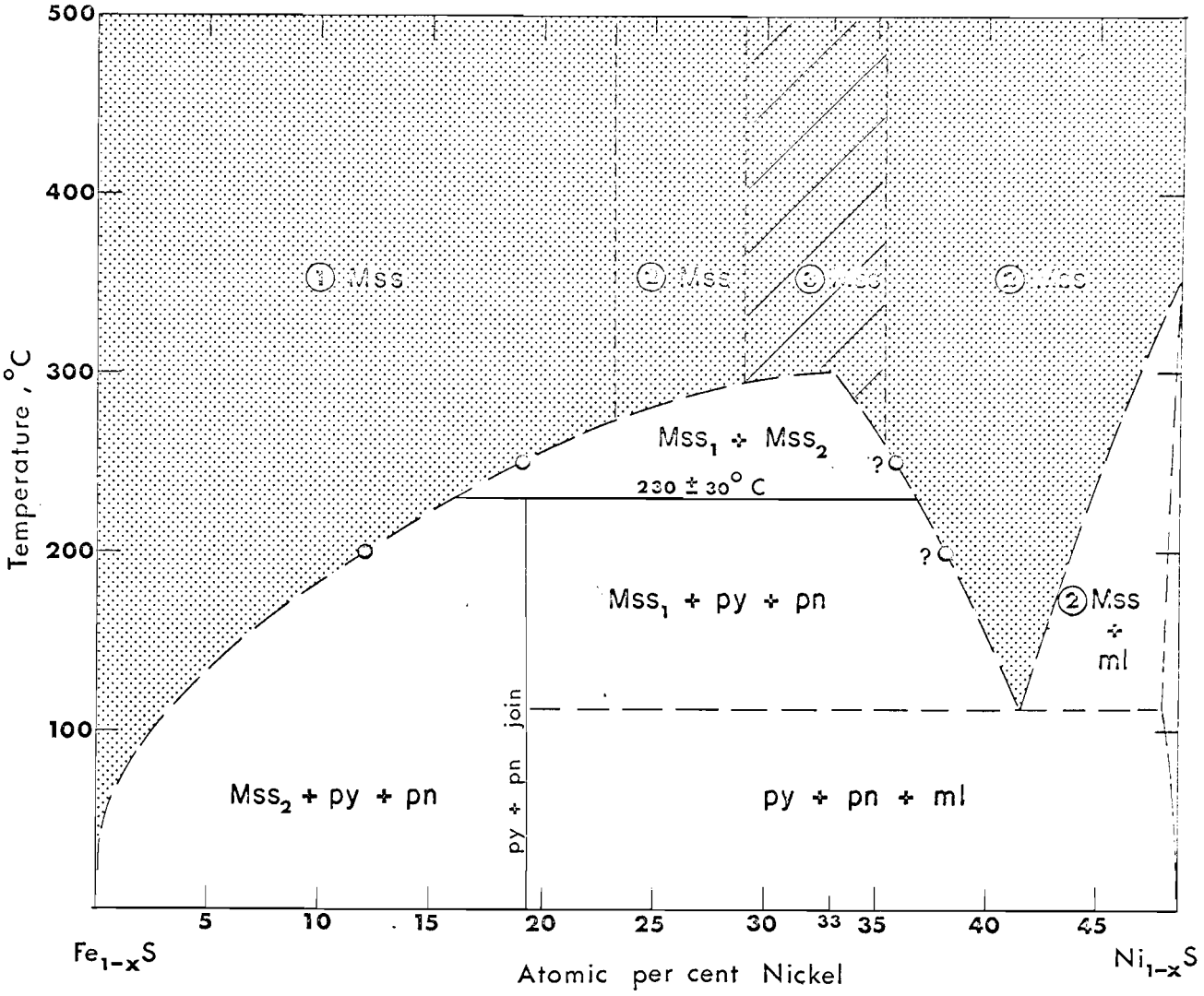

Figure 11. Generalized, semi-schematic section along an $Fe_{1-x}S$ - $Ni_{1-x}S$ join.

① Mss= Monosulphide solid solution that shows pyrrhotite-type structure modified by supercell reflections when cooled to room temperature.

② Mss= Monosulphide solid solution that shows NiAs - type structure when cooled to room temperature.

③ Mss= Zone corresponding to the steep portions of d_{102} - composition curves (Fig. 6) and including the monosulphide solid solution modulated structure at 33 atomic per cent nickel.

Solid circles represent solvus limits determined in this study.

which, in the case of pyrrhotite, is still under intensive investigation by many workers. The phase relations shown in Figure 11 in the immediate vicinity of the end members have been simplified for clarity and do not necessarily represent the exact phase relations for any section between $Fe_{1-x}S$ and $Ni_{1-x}S$. The phase relations in the central portion of the section are relatively simple and are thought to be consistent for any section between $Fe_{1-x}S$ and $Ni_{1-x}S$. Immiscibility within the Mss field is rather abrupt and is perhaps complete within the temperature range 300 to 150°C. The upper limit of the region in which the Mss modulated structure occurs remains to be defined.

CHAPTER V

GEOLOGICAL APPLICATION OF EXPERIMENTAL RESULTS

The phase relations in the synthetic Fe-Ni-S system were determined in the presence of vapor, thus the results are theoretically only applicable to the natural phases when vapor is present. Although the environment of ore deposition is chemically much more complex than the system studied, the composition and stability of the phases in equilibrium is effected only by those components in the natural environment that enter into the composition of the minerals formed. Knop and Ibrahim (1961) have shown that the substitution of Co for Fe and Ni in pentlandite has little effect on the solubility limits of pentlandite. In general, if the amount of substitution is small, the effect on the equilibrium will usually also be small (Kullerud, 1959).

Pentlandite

An interesting anomaly exists between the range in composition of synthetic and natural pentlandites. The iron and nickel solubility limits of synthetic pentlandite are much greater than the range in composition of natural pentlandite as found by Knop et al. (1965). A peculiarity of natural pentlandites is the apparent uniformity in composition from a single ore deposit and frequently from one mining district. The solution to these paradoxes is not evident from this study, but some suggestions

can be made as to future methods of attack on the problem. Synthetic studies below 400°C may well show that the pentlandite solubility field decreases considerably at lower temperatures, or an electron probe analysis of natural pentlandite may reveal some variation in the chemical composition that may more closely correspond to the range in composition of synthetic pentlandite.

An x-ray method for the determination of the nickel and iron content of natural pentlandites was tested using pentlandite from the Creighton mine, Sudbury (McGill sample No. E410), and from the Marbridge mine, Quebec (L. A. Clark sample No. 4-2). Coarse-grained pentlandite was carefully hand-separated from single hand specimens, but some impurities, largely pyrrhotite, were present in the separated fractions. About 100 mg. of the pentlandite concentrate from each sample was annealed at 400°C for three days in sealed, evacuated, silica glass tubes. The annealing procedure was necessary as the lattice parameter of natural pentlandite is significantly different from that of synthetic pentlandite (Knop et al. 1965). After quenching, the d_{115} value was measured using Li F as an internal standard. As the determinative curve (Figure 5) is theoretically only applicable to pentlandite coexisting with γ(Fe, Ni), the measured d_{115} value had to be adjusted in order that the determinative curve could be used for pentlandites coexisting with pyrrhotite. The average change in d - value

(+0.0033 Å) found in crossing the pentlandite field on the Fe : Ni = 1 : 1 section was used to correct the measured d_{115} values. After applying the correction, the Fe : Ni weight ratio was determined from Figure 5. The Creighton and Marbridge pentlandites were found to have Fe : Ni weight ratios of 1.15 and 1.13 respectively. Analysis of Creighton pentlandite (compiled by Knop et al., 1965) show Fe : Ni weight ratio values of 0.83 to 0.88. The discrepancy between the x-ray and chemically determined composition of Creighton pentlandite cannot be completely resolved at this time. One source of error is in the assumption that the correction applied to the determinative curve is constant for the complete range in composition of pentlandite. The annealing of natural pentlandites may introduce another error due to some change in the composition of pentlandite on heating. In spite of the discrepancy found, the application of the x-ray determinative curve to natural pentlandites cannot be disregarded until more natural pentlandites, particularly pentlandites having large compositional differences from the Creighton and Marbridge pentlandites, are investigated and the writer's results substantiated.

Pyrite-Pentlandite Assemblages

The experimental study has established that pyrite and pentlandite cannot coexist above 230 ± 30°C in the presence of their equilibrium vapor. Although either mineral can form at higher temperatures, their

occurrence together in an ore deposit indicates that at least one of them formed below 230°C. This stability limit may increase with increased confining pressure (Kullerud, 1959).

Pentlandite - Ni_7S_6 Assemblages

The experimental study has established that a tie line between pentlandite and Ni_7S_6 is present at 500 and 400°C, which would suggest that the phase Ni_7S_6 should occur frequently as a mineral and that millerite and heazlewoodite are not compatible. However, Ni_7S_6 is not reported as a mineral. This may be in part due to the difficulty in distinguishing Ni_7S_6 from millerite in polished sections. The occurrence of the heazlewoodite plus millerite assemblage at a number of localities is well documented (Kullerud and Yund, 1962), but where they occur, millerite formation was a secondary process. Thus, if the alteration of heazlewoodite produces millerite, Ni_7S_6 should appear as the first product of heazlewoodite alteration and should be searched for at localities where such conditions exist. Ni_7S_6 should also be looked for at localities where primary millerite occurs and where the f_{S_2} was low enough for Ni_7S_6 to form.

CHAPTER VI

CONCLUSIONS

The major conclusions of this study may be summarized as follows:

1. Pentlandite synthesized at 500 and 400°C has a much greater solubility of iron and nickel than naturally occurring pentlandites and the previously reported synthetic pentlandites.
2. Pyrite and pentlandite cannot coexist above 230 ± 30°C in the presence of their equilibrium vapor.
3. Monosulphide solid solution synthesized at 500 and 400°C with a composition of about 33 atomic per cent nickel forms a modulated structure which is an intermediate step prior to the formation of two immiscible phases.

Suggestions for Further Work

1. Synthetic studies on the iron and nickel solubility limits of pentlandite below 400°C should be attempted to determine if the homogeneity field decreases markedly. This would help to explain the narrow composition limits of natural pentlandites.

Excessively long equilibration times may make this study impractical with existing experimental techniques.

2. An election probe study of natural pentlandites to determine if there is any variation in the chemical composition within a single ore deposit is warranted.
3. Further investigation into the applicability of the x-ray determinative curve to natural pentlandites is warranted. The determinative curve should first be tested with natural pentlandites that have compositions significantly different from that of the Sudbury and Marbridge pentlandites used in this study.
4. The upper stability limit of the pyrite-pentlandite assemblage should be confirmed by studying the reaction pyrrhotite + millerite $\rightleftharpoons$ pyrite + pentlandite.
5. A crystallographic investigation into the Mss series to determine the variation of the cell constants with composition would help to interpret the nature of the solid solution and the development of the modulated structure. A full interpretation of the crystal chemistry of Mss would necessitate single - crystal studies which may prove to be difficult as the ability to synthesize single - crystals of Mss has not been demonstrated.

References

Alsén, N. (1925) Rontgenographische Untersuchung der Kristallstrukturen von Magnetkies, Breithauptit, Pentlandit, Millerit und verwandten Verbindungen. Geol. Foren. Forhandl. 47, 54.

Arnold, R.G., and Kullerud, G. (1956) The NiS-NiS_2 Join. Carnegie Inst. Wash. Year Book 55, 178-180.

Arnold, R.G. (1962) Equilibrium relations between pyrrhotite and pyrite from 325 to 743°C. Econ. Geol. 57, 72-90.

Bell, P.M., England, J.L., and Kullerud, G. (1964) Pentlandite, Pressure Effect on Breakdown. Carnegie. Inst. Wash. Year Book 63, 206-207.

Berry, L.G., and Thompson, R.M. (1962) X-ray powder data for ore minerals: The Peacock Atlas. Geol. Soc. Am. Mem. 85.

Bornemann, K. (1908) Schmelzdiagramm der Nickel-Schwefelverbindungen. Metallurgie 5, 13-19.

_____ (1910) Das System Nickel-Schwefel. II. Mitteilung. Ibid. 7, 667-674.

Bradley, A.J. (1940) X-ray evidence of intermediate stages during precipitation from solid solution. Proc. Phys. Soc. London, 52, 80-85.

Cabri, L.J. (1964) Phase relations in the Au-Ag-Te System. Unpubl. Ph.D. thesis, McGill University, Montreal, Canada.

Clark, L.A. (1959) Phase relations in the Fe-As-S System. Unpubl. Ph.D. thesis, McGill University, Montreal, Canada.

_____ and Kullerud, G. (1963) The sulphur-rich portion of the Fe-Ni-S system. Econ. Geol., 58, 853-885.

_____ (1965) Personal communication.

Colgrove, G.L. (1940) The FeS-NiS System. Unpubl. M.A. thesis, Queen's University, Kingston, Canada.

_____ (1942) The system Fe-Ni-S. Unpubl. Ph.D. thesis, University of Wisconsin.

Desborough, G.A., and Carpenter, R.H. (1965) Phase relations of pyrrhotite. Econ. Geol., 60, 1431-1450.

Dickson, C.W. (1903) The ore deposits of Sudbury. Trans. Am. Inst. Min. Eng., 34, 3-67.

Eliseev, E.N. (1955) O sostave i kristallicěskoj strukture pentlandita. Zap. Vsesoj. Mineral. Obšč., 84, 53-62.

Elliott, P.R. (1965) Constitution of binary alloys, first supplement. McGraw-Hill, 422-423.

Géller, S. (1962) Refinement of the crystal structure of Co_9S_8. Acta Cryst., 15, 1195.

Guertler and Savelsberg. (1932) Metall. und Erz., 5, 84.

Guinier, A. (1963) X-ray Diffraction in crystals, imperfect crystals and amorphous bodies. W.H. Freeman and Co., 378 p.

Hansen, M., and Anderko, K. (1958) Constitution of binary alloys. McGraw-Hill, 677-684.

Hawley, J.E. (1962) The Sudbury ores: Their mineralogy and origin. Can. Mineral., 7, 207 pp.

Knop, O., and Ibrahim, M.A. (1961) Chalkogenides of the Transition elements. II. Existence of the π phase in the M_9S_8 section of the system Fe-C0-Ni-S. Can. J. Chem., 39, 297-317.

Knop, O., Ibrahim, M.A., and Sutarno. (1965) Chalcogenides of the Transition elements. IV. Pentlandite, a natural π phase. Can. Mineral., 8, 291-316.

Kullerud, G. (1956) Subsolidus phase relations in the Fe-Ni-S system. Carnegie Inst. Wash. Year Book, 55, 175-177.

_____ (1959) Sulphide systems as geological thermometers: In Researches in Geochemistry, ed. P.H. Abelson, Wiley, N.Y., 301-335.

_____, and Yoder, H.S. (1959) Pyrite stability relations in the Fe-S system. Econ. Geol., 54, 533-572.

_____, and Yund, R.A. (1962) The Ni-S system and related minerals. J. Petrology, 3, 126-175.

_____ (1963) The Fe-Ni-S system. Carnegie Inst. Wash. Year Book, 62, 175-189.

_____ (1963) Thermal stability of pentlandite. Can. Mineral., 7, 353-366.

Lindqvist, M., Lundqvist, D., and Westgren, A. (1936) The crystal structure of Co_9S_8 and of pentlandite $(Ni,Fe)_9S_8$. Kemisk Tidskrift, 48, 156-160.

Lundqvist, D. (1947) X-ray studies on the ternary system Fe-Ni-S. Arkiv, Kemi. Min. Geol., 24, no. 22, 1-12.

Morimoto, N., and Kullerud, G. (1964) Pentlandite, Thermal Expansion. Carnegie Inst. Wash. Year Book, 63, 204-205.

Newhouse, W.H. (1927) The equilibrium relations of pyrrhotite and pentlandite. Econ. Geol., 22, 288-299.

Pearson, A.D., and Buerger, M.J. (1956) Confirmation of the crystal structure of pentlandite. Am. Min., 41, 804-805.

Penfield, S.L. (1893) On pentlandite from Sudbury, Ontario. Am. Jour. Sci., 45, 492-497.

Popova, G.B., Yershov, V.V., and Kuznetsov, V.A. (1964) Experimental study of the fusion and crystallization of pentlandite. Doklady Akad. Nauk SSSR, 156, 114-118.

Roberts, H.S. (1935) Polymorphism in the FeS - S solid solutions. I. Thermal Study. Jour. Am. Chem. Soc., 57, 1034-1038.

Scheerer, Th. (1843) Ueber ein neues Vorkommen des Nickels. Ann. Phys., 58, 315-319.

Taylor, A. (1961) X-ray Metallography, John Wiley and Sons, Inc., 507-512.

Urazov, G.G., and Filin, N.A. (1938) Investigation of the ternary iron-nickel-sulphur system. Metallurg. 13, No.2, 3-17.

Vogel, R., and Tonn, W. The ternary system Fe-Ni-S. Archiv. fur das Eisenhuttenwesen, 12, 769-780.

Zurbrigg, H.F. (1933) A study of nickeliferous pyrrhotite. Unpubl. M.Sc. thesis, Queen's University, Kingston, Ontario.

APPENDIX

TABLE A 1

DETERMINATION OF SULPHUR SOLUBILITY ON EITHER SIDE OF $Fe_{4.5}Ni_{4.5}S_8$ (33.23 wt %S)

Run No.	wt % S	Time (days)	Products	d_{115} of pentlandite Å
	(a) 600°C			
193	31.09	11.6	pn + Mss + $(Ni, Fe)_{3 \pm x}S_2$	1.9465
194	31.99	11.6	pn + Mss + $(Ni, Fe)_{3 \pm x}S_2$	1.9481
183	32.52	12.9	pn	1.9462
195	32.77	11.6	pn + Mss	1.9464
180	33.10	19.6	pn + Mss	1.9452
184	33.27	12.9	pn + Mss	1.9446
185	33.47	12.9	pn + Mss	1.9442
186	34.02	12.9	pn + Mss	1.9428
196	35.12	11.6	pn + Mss	1.9428
	(b) 500°C			
39	30.13	40.2	pn + γ(Ni, Fe)	1.9466
65	31.12	10.0	pn + γ(Ni, Fe)	1.9467
31	32.02	10.9	pn + γ(Ni, Fe)	1.9463
67	32.62	11.3	pn + γ(Ni, Fe)	1.9458
85	32.78	39.0	pn + γ(Ni, Fe)	1.9462
86	32.92	39.0	pn + γ(Ni, Fe)	1.9461
87	33.01	39.0	pn + γ(Ni, Fe)	1.9461
88	33.10	36.9	pn + Mss	1.9454
13	33.24	3.8	pn + Mss	1.9456
14	33.28	19.6	pn + Mss	1.9455
66	33.38	11.9	pn + Mss	1.9441
68	33.51	11.9	pn + Mss	1.9446
145	33.61	19.7	pn + Mss	1.9439
146	33.72	19.7	pn + Mss	1.9440
147	33.82	19.7	pn + Mss	1.9435

Continued Table A 1

34	34.08	67.8	pn + Mss	1.9431
89	35.01	36.9	pn + Mss	1.9430
35	35.27	84.9	pn + Mss	1.9430
36	36.19	47.3	pn + Mss	1.9432
	(c) 400°C			
69	30.03	14.4	pn + γ(Ni, Fe) + hz*	1.9476
155	31.03	40.8	pn + γ(Ni, Fe)	1.9473
25	31.99	34.8	pn + γ(Ni, Fe) + hz*	1.9466
156	32.33	40.8	pn + γ(Ni, Fe)	1.9463
70	32.58	14.5	pn + γ(Ni, Fe) + hz*	1.9468
90	32.70	40.1	pn + γ(Ni, Fe) + hz*	1.9463
91	32.78	40.1	pn + γ(Ni, Fe) + hz*	1.9464
92	32.90	40.1	pn + γ(Ni, Fe) + hz*	1.9459
71	32.97	14.5	pn	1.9459
4	33.19	8.7	pn + Mss + hz*	1.9449
18	33.23	39.0	pn + Mss	1.9449
19	33.30	42.9	pn + Mss + hz*	1.9444
22	33.99	37.0	pn + Mss	1.9433
23	34.99	37.0	pn + Mss	1.9427
24	36.04	36.0	pn + Mss	1.9423

*Equilibrium not attained

APPENDIX

TABLE A 2

DETERMINATION OF THE IRON AND NICKEL SOLID SOLUBILITY LIMITS OF PENTLANDITE WITH ABOUT 33.05 WEIGHT PER CENT SULPHUR

Run No.	wt % Fe	wt % Ni	Fe : Ni wt ratio	Time (days)	Products	d_{115} of pn Å
		(a) 600°C				
157	43.95	22.97	1.914	20.9	pn + Mss + $(Ni, Fe)_{3 \pm x}S_2$	1.9483
158	38.94	28.02	1.390	20.9	pn + Mss + $(Ni, Fe)_{3 \pm x}S_2$	1.9476
164	36.20	30.76	1.177	20.5	pn + Mss + $(Ni, Fe)_{3 \pm x}S_2$	1.9477
179	34.74	32.21	1.078	19.6	pn + Mss	1.9465
159	33.26	33.69	0.987	20.9	pn + Mss	1.9467
180	32.55	34.35	0.948	19.6	pn + Mss	1.9452
181	31.68	35.22	0.900	19.6	pn + Mss	1.9447
182	30.62	36.31	0.8435	19.6	pn + Mss	1.9449
163	29.61	37.32	0.794	20.5	pn + Mss	1.9431
192	27.60	39.34	0.702	15.9	pn + Mss	1.9437
191	24.58	42.39	0.580	15.9	pn + Mss + $(Ni, Fe)_{3 \pm x}S_2$	1.9422
160	22.18	44.78	0.4953	20.9	pn + Mss + $(Ni, Fe)_{3 \pm x}S_2$	1.9424
		(b) 500°C				
144	47.48	19.43	2.444	22.0	pn + Mss + γ(Ni, Fe)	1.9586
143	45.30	21.64	2.093	22.0	pn + Mss + γ(Ni, Fe)	1.9583
142	43.16	23.80	1.813	22.0	pn + Mss + γ(Ni, Fe)	1.9582
141	41.19	25.73	1.601	22.0	pn	1.9571
137	39.07	27.90	1.400	17.0	pn	1.9531
136	37.86	29.12	1.300	17.0	pn	1.9511
127	36.61	30.35	1.206	26.8	pn	1.9492
124	35.01	31.90	1.097	26.3	pn	1.9473
123	33.32	33.61	0.991	26.3	pn	1.9458
122	31.27	35.63	0.877	26.3	pn	1.9447
121	29.77	37.17	0.801	26.3	pn	1.9443
126	27.16	39.73	0.684	26.8	pn	1.9429

Continued TABLE A 2

125	24.96	41.96	0.595	26.8	pn	1.9420
139	22.27	44.64	0.499	17.0	pn + Mss	1.9414
138	19.06	47.84	0.398	17.0	pn + Mss	1.9400
174	15.53	51.41	0.302	14.3	pn + Mss + $\propto Ni_7S_6$	1.9399
175	14.01	52.89	0.265	14.3	pn + Mss + $\propto Ni_7S_6$	1.9402
173	11.10	55.84	0.199	14.3	pn + Mss + $\propto Ni_7S_6$	1.9404
176	5.94	60.98	0.098	14.3	pn + Mss + $\propto Ni_7S_6$	1.9392

(c) 400°C

187	47.64	19.32	2.466	32.0	pn + Mss + γ(Ni, Fe)	1.9659
198	45.73	21.20	2.157	61.7	pn + Mss + γ(Ni, Fe)	1.9671
149	44.68	22.25	2.008	41.0	pn + Mss + γ(Ni, Fe)	1.9642
197	43.11	23.81	1.811	61.7	pn + γ(Ni, Fe)	1.9625
188	42.00	24.88	1.688	32.0	pn + γ(Ni, Fe)	1.9592
150	39.95	26.99	1.480	41.0	pn + γ(Ni, Fe)	1.9534
153	36.55	30.41	1.202	40.8	pn + γ(Ni, Fe)	1.9487
151	33.35	33.61	0.992	41.0	pn	1.9465
71	32.67	34.36	0.952	14.5	pn	1.9459
154	29.55	37.35	0.791	40.8	pn	1.9436
161	26.84	40.11	0.669	40.3	pn	1.9425
152	22.32	44.64	0.500	41.0	pn + Mss	1.9427
190	12.98	53.92	0.241	32.0	pn + Mss + $\propto Ni_7S_6$	1.9417
189	6.95	60.00	0.116	32.0	pn + Mss + $\propto Ni_7S_6$	1.9419

APPENDIX

TABLE A 3

RESULTS OF MONOSULPHIDE SOLID SOLUTION STUDY

Run No	wt % Fe	wt % Ni	wt % S	Time (days)	Products Remarks	d_{102}, Å
			(a) 500°C			
109	54.67	16.16	39.17	23.8	Mss, pyrrhotite-type structure	2.0541
113	50.75	10.28	38.97	24.2	Mss, pyrrhotite-type structure	2.0516
93	48.80	12.24	38.96	12.0	Mss, pyrrhotite-type structure	2.0439
110	46.00	15.27	38.73	23.8	Mss, pyrrhotite-type structure	2.0444
94	42.89	18.51	38.59	12.0	Mss, pyrrhotite-type structure	2.0415
104	39.36	22.23	38.41	8.8	Mss, pyrrhotite-type structure	2.0388
95	36.89	24.81	38.30	12.0	Mss, NiAs-type structure	2.0376
96	30.78	31.21	38.01	13.8	Mss, NiAs-type structure	2.0283
112	24.88	37.39	37.73	23.8	Mss, NiAs-type structure	2.0241
172	23.28	39.11	37.61	17.7	Mss, NiAs-type structure	2.0205
171	21.99	40.45	37.56	17.7	Mss, NiAs-type structure	2.0165
170	20.41	42.12	37.47	17.7	Mss, NiAs-type structure	2.0137
114	18.76	43.80	37.44	24.2	Mss, modulated structure	2.0106
169	17.50	45.16	37.34	17.7	Mss, NiAs-type structure	2.0017
166	16.14	46.59	37.27	17.7	Mss, NiAs-type structure	1.9991
167	9.97	53.06	36.97	17.7	Mss, NiAs-type structure	1.9931
116	6.30	56.91	36.79	24.2	Mss, NiAs-type structure	1.9896
168	3.15	60.20	36.65	17.7	Mss, NiAs-type structure	1.9879
165	- -	63.51	36.49	17.7	$Ni_{1-x}S$, NiAs-type structure	1.9840

Continued TABLE A 3

(b) 400°C

117	54.11	6.73	39.16	29.0	Mss, pyrrhotite-type structure	2.0557
132	52.87	8.07	39.06	34.5	Mss, pyrrhotite-type structure	2.0531
133	50.80	10.25	38.95	34.5	Mss, pyrrhotite-type structure	2.0495
134	48.83	12.26	38.91	34.5	Mss, pyrrhotite-type structure	2.0484
97	47.95	13.20	38.85	37.8	Mss, pyrrhotite-type structure	2.0478
135	45.89	15.41	38.70	34.5	Mss, pyrrhotite-type structure	2.0457
98	43.01	18.40	38.59	37.8	Mss, pyrrhotite-type structure	2.0417
101	39.75	21.78	38.47	35.7	Mss, pyrrhotite-type structure	2.0379
99	36.98	24.73	38.29	37.8	Mss, NiAs-type structure	2.0347
102	33.99	27.87	38.14	35.7	Mss, NiAs-type structure	2.0326
100	30.92	31.06	38.02	37.8	Mss, NiAs-type structure	2.0287
103	24.91	37.38	37.70	35.7	Mss, NiAs-type structure	2.0228
118	18.78	43.83	37.39	29.0	Mss, modulated structure	2.0045
119	12.58	50.31	37.11	29.0	Mss, NiAs-type structure	1.9957
120	6.30	56.89	36.81	29.0	Mss, NiAs -type structure	1.9898

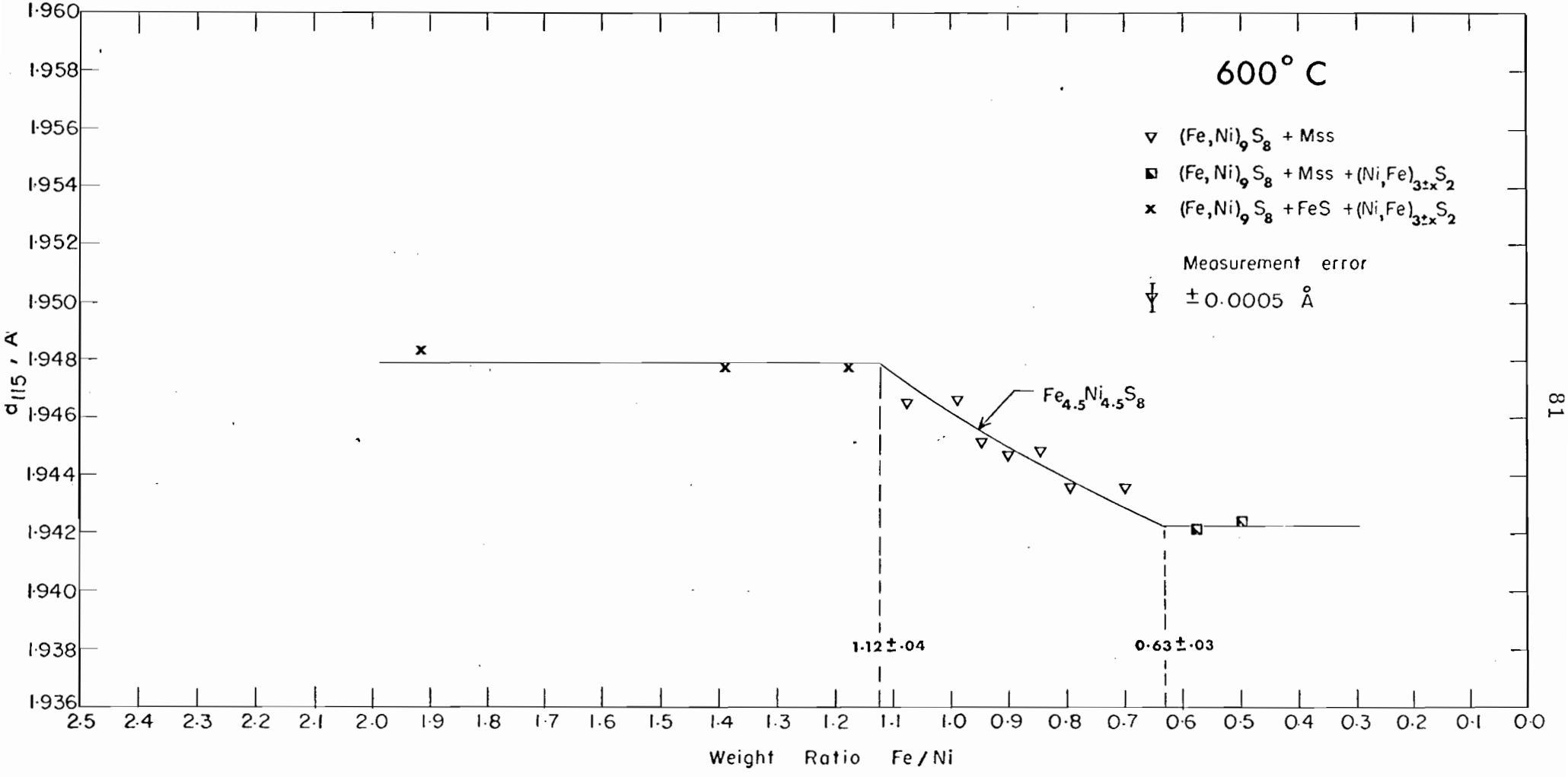

Figure A1. Variation in the d_{115} of pentlandite as a function of the Fe : Ni weight ratio along a section of 33.05 weight per cent S at 600°C. All phases coexist with vapor.

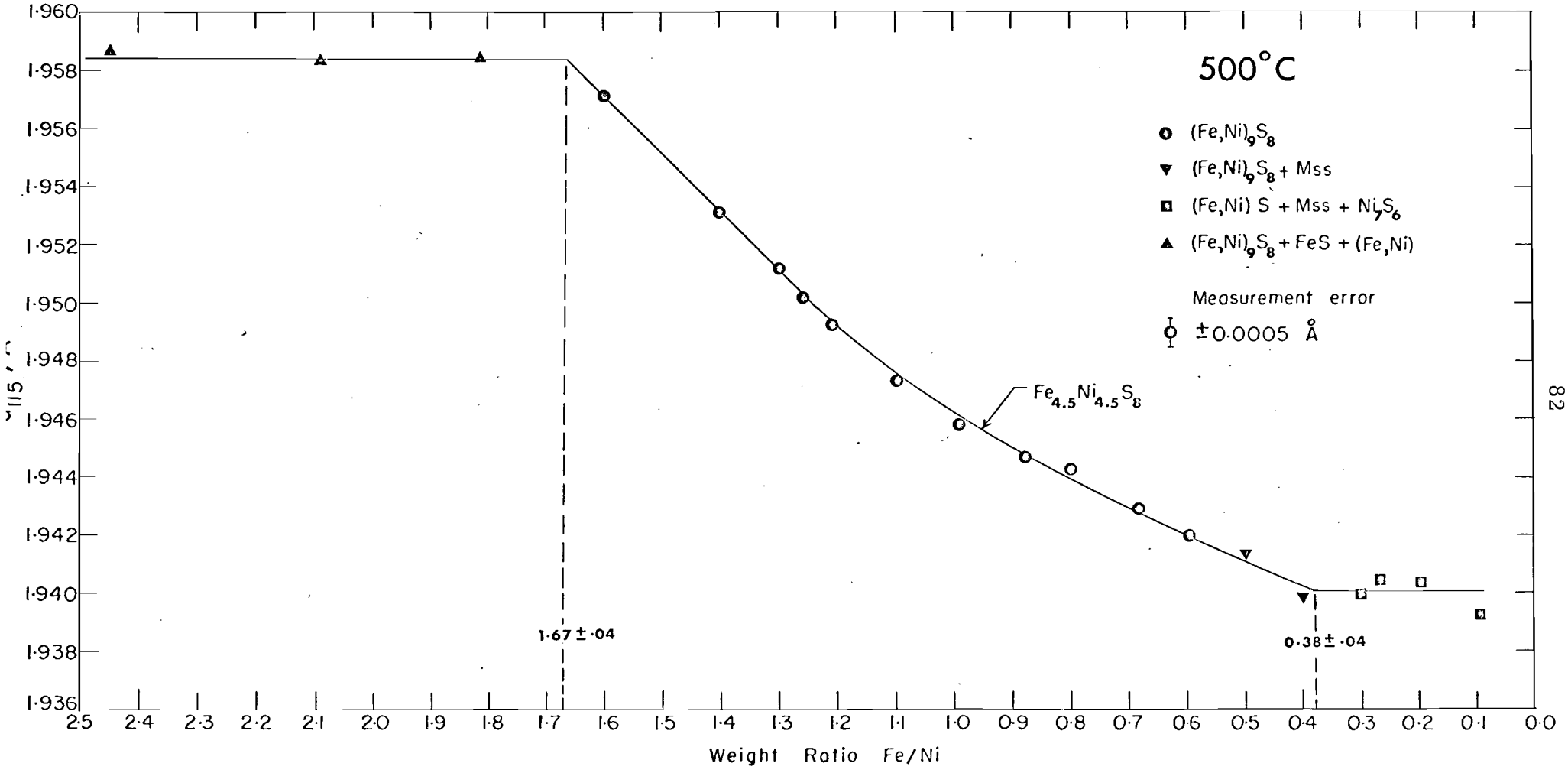

Figure A2. Variation in the d_{115} of pentlandite as a function of the Fe : Ni weight ratio along a section of 33.05 weight per cent S at 500°C. All phases coexist with vapor.

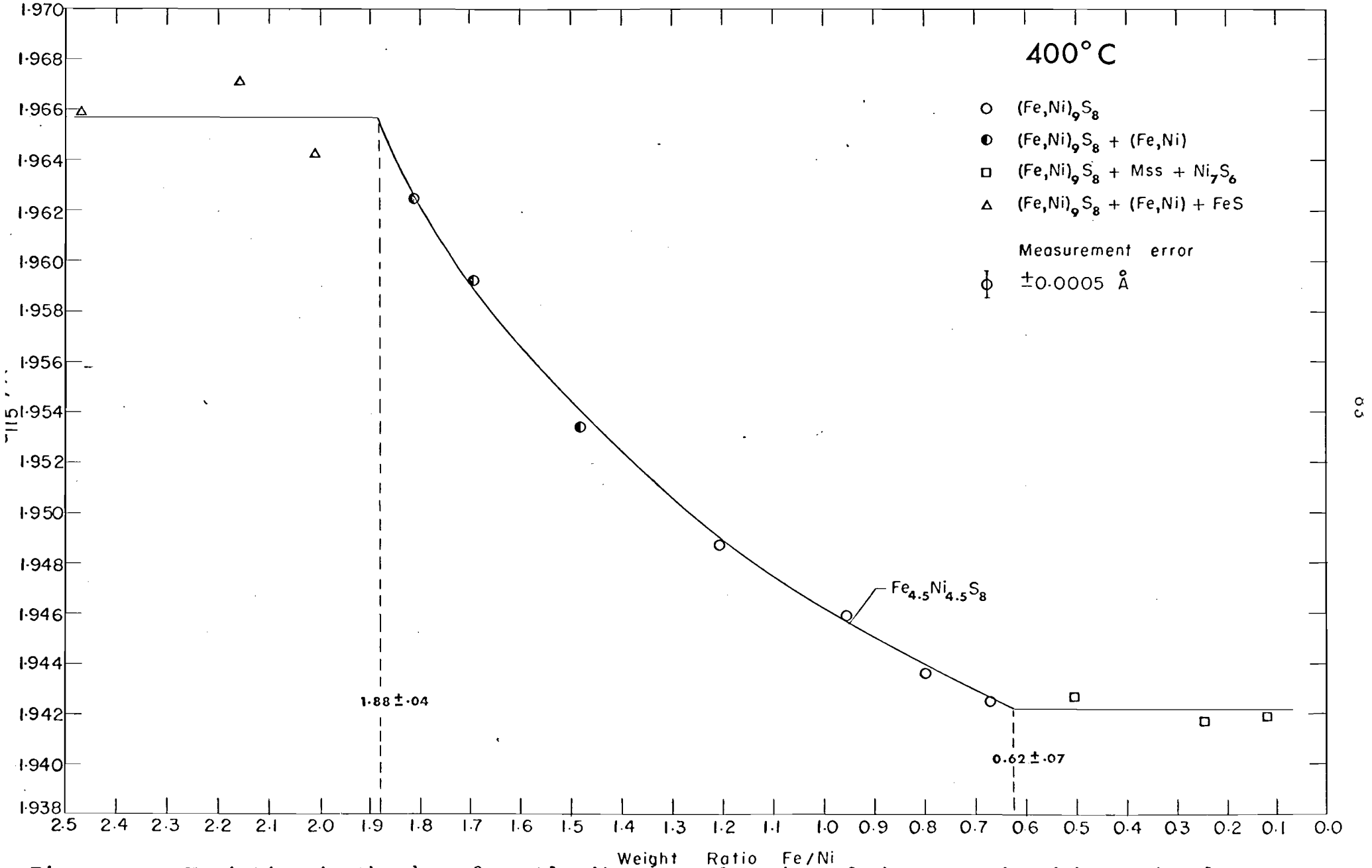

Figure A3. Variation in the d_{115} of pentlandite as a function of the Fe : Ni weight ratio along a section of 33.05 weight per cent S at 400°C. All phases coexist with pyrrh